Silk Electrogel Based Gastroretentive Drug Delivery System

A thesis submitted by

Qianrui Wang

In partial fulfillment of the requirements

for the degree of

Master of Science

in

Biomedical Engineering

TUFTS UNIVERSITY

SCHOOL OF ENGINEERING

February 2015

Academic Adviser: Professor David L. Kaplan, Ph.D.

Department committee member: Professor Qiaobing Xu, Ph.D.

Cross department committee member: Professor Kyongbum Lee, Ph.D.

ABSTRACT

Gastric cancer has become a global pandemic and there is imperative to develop efficient therapies. Oral dosing strategy is the preferred route to deliver drugs for treating the disease. Recent studies suggested silk electro hydrogel, which is pH sensitive and reversible, has potential as a vehicle to deliver the drug in the stomach environment. The aim of this study is to establish in vitro electrogelation *e*-gel based silk gel as a gastroretentive drug delivery system. We successfully extended the duration of silk e-gel in artificial gastric juice by mixing silk solution with glycerol at different ratios before the electrogelation. Structural analysis indicated the extended duration was due to the change of beta sheet content. The glycerol mixed silk e-gel had good doxorubicin loading capability and could release doxorubicin in a sustained-release profile. Doxorubicin loaded silk e-gels were applied to human gastric cancer cells. Significant cell viability decrease was observed. We believe that with further characterization as well as functional analysis, the silk e-gel system has the potential to become an effective vehicle for gastric drug delivery applications.

ACKNOWLEDGEMENT

I am grateful to Professor David Kaplan for giving me the opportunity to pursue my research at Tufts University, to all members in the Kaplan lab for all the support during study, and to my family, my friends, and my girlfriend Juan Wang who always encourage and concern me.

Qianrui Wang

TABLE OF CONTENTS

.

LIST OF TABLES

LIST OF FIGURES

CHAPTER 1

INTRODUCTION

1.1. Background

Adenocarcinoma of the stomach is the 3rd leading cause of cancer death worldwide, responsible for 989,600 new cases and 738,000 deaths annually.[1] More than 80% of these cases been assigned to to *H.Pylori* infection.[2] This is a gram-negative microaerophilic, spiral bacterium found in the gastric mucosa in patients with severe gastritis and chronic atrophic gastritis. Other common causes of the stomach cancer include eating pickled vegetables, and smoking. The case-fatality ratio of gastric cancer is larger than for common malignancies like colon, breast, and prostate cancers worldwide, which makes it a fatal disease.[3] The main reasons for this high death rate are its vague and nonspecific symptoms in early infection stages and the resistance of *H. Pylori* to eradication in gastric mucosa.[4] The current therapy for the treatment of gastric adenocarcinoma involves the use of proton pump inhibitors with antibiotics and has drawbacks like poor patient compliance and increased bacterial resistance due to higher multiple doses of antibiotics.[5] Thus, developing a gastric retentive drug delivery system to increase the drug residence time in the stomach is one approach to improve the efficacy of therapy.[6]

Silk fibroin protein from *Bombyx mori*, the commercialized source of silk for textiles via sericulture, is a promising material for drug delivery due to the aqueous processing ability, biocompatibility and biodegradability.[7] The molecular structure of *B. mori* silk, consists of large regions or domains of hydrophobic amino acids, segregated by relatively short and more hydrophilic regions.[8] The hydrophobic domains organize into protein

crystals, beta sheets, which form physical crosslinks to stabilize silk structures. These regions are characterized by repeats of alanine, glycine-alanine, or glycine-alanine-serine. By monitoring the degree of crystalline beta-sheet formation, silk can exhibit high encapsulation efficiency and controllable drug release kinetics.[7] Electro silk hydrogel, which can be formed through weak electric fields from silk aqueous solution,[9] was studied for drug delivery applications in the stomach. This was selected due its hydrophilic and three-dimensional network structure helps to encapsulate and regulate the release of drugs, and since its sensitiveness to pepsin digestion unlike ordinary induced silk hydrogels.

1.2. Stomach cancer

Cancer annually accounts for 12.2 percent of total deaths worldwide, and cancers of the stomach are among the most frequent gastrointestinal tract cancers, irrespective of gender or regional-specific variations.[3]

Stomach cancer, also called gastric cancer, is a cancer that starts in the stomach. The word stands for a malignant tumor arising from the lining of the stomach. This disease is the fourth most commonly diagnosed cancer and is the second leading cause of cancer death worldwide according to a report written by the World Health Organization in 2009. It is also of the view that stomach cancers account for 989 600 new cases and 738 000 deaths annually.[10] In US, the NCI predicts that 21,600 Americans will get this disease and 10,990 of them will die of the disease in 2014.[11] The 5 year survival rate is as low as 25.7%, which has not significantly changed during the past 40 years.[12]

1.2.1. Gastric cancer: disease etiology

Gastric cancer is a multifactorial disease, the incidence and mortality rates of stomach cancer vary by race/ethnicity, sex and by nation. Researchers believe this difference is caused by the variance of diet, lifestyle, genes, socioeconomic and other factors.[13]

Among various factors, *H. pylori* has been classified as a group one carcinogen by the World Health Organization since more than 80% of cases have been attributed to *H. Pylori* infection.[14] In 1994, the International Agency for Research on Cancer categorized *H. pylori* as a "Group one human carcinogen" based on a plethora of studies.[15] *H. Pylori* is a gram-

negative microaerophilic, spiral bacterium found in the gastric mucosa in patients with severe gastritis and chronic atrophic gastritis.[4] In a prospective study in Japan, 2.9% of *H. pylori* infected patients subsequently developed gastric cancer while none of the uninfected patients developed tumors.[16] The results of several meta-analyses concluded that *H. pylori* infection is associated with an approximate 2-7 fold increased risk of developing gastric cancer.[16-17]

H. Pylori triggers a cascade of bio events that promote the sequential progression gastric epithelium through atrophic gastritis, intestinal metaplasia, and dysplasia to carcinoma.[18]

1.2.2. Gastric cancer: disease epidemiology

Stomach cancer was the leading cause of cancer-related death in the US in 1930. Since then on, it has decreased by more than 80%. Similar trends have been found in countries with historically high stomach cancer incidence rates including China, Korea, Ecuador and Japan.[19]

The reasons for this worldwide decline are not well understood although many researchers suggest that it may be due to the decreased reliance on salted and preserved foods, and also because the increased availability of fresh fruits and vegetables since the invention of the refrigerator since 1930s.[14]

Reduction in the use of tobacco may also contribute to the decrease in stomach cancer incidence rates in the United States, the United Kingdom, and other Western countries, where the tobacco epidemic has long been established.[20]

1.2.3. Gastric cancer: current treatment and limitations

Four types of standard treatments include surgery,[21] chemotherapy,[22] radiation therapy and immunotherapy are used in order to treat gastric cancer based on the recommendation of the National Cancer Institute. Although surgical resection is the only clinical method to eradicate localized gastric cancer, adjuvant therapies like chemotherapy can help increase the 5 year survival rate significantly in treated patients when administered prior to and after surgery.[23] A meta-analysis by the global advanced/adjuvant stomach tumor research international collaboration group in 2010 demonstrated that adjuvant chemotherapy leads to a 6% increase in the 5-year overall survival rate compared with surgical treatment alone.[24] However, chemotherapy is usually taken by mouth or injected into a vein or muscle, which create systemic drug concentrations of the whole body and results in difficulty of maintaining effective drug concentration levels in the stomach. This also results in uncontrollable toxic side-effects in healthy tissues. Thus, there exists an urgent need to improve the survival rate of stomach cancer patients by developing a gastroretentive drug delivery system which can improve an anticancer drugs' therapeutic outcome.

1.3. GI tract and gastroretentive drug delivery systems

The human gastrointestinal tract/GI tract is a system which is responsible for consuming and digesting foodstuffs, absorbing nutrients, and expelling waste (Fig 1.a). It is considered a preferred route to deliver drugs because of the low cost of therapy, ease of administration and patient compliance.

At present, however, oral dosing strategies are limited to pharmaceutical agents that have acceptable oral bioavailability. One issue that directly impacts oral bioavailability/ efficiency of orally administered dosage forms is the residence time of the drug formulation at the desired site of action. The complex anatomy and physiology of the GI tract (variations in pH gradient, complicated bile salts, enzyme content, and the mucosal absorptive surface) affect the dissolution, release and uptake of orally administered dosage forms and consequently, limit the contact time between the drug dosage and mucus membrane. Similarly, drugs which produce their local action in the stomach are rapidly emptied and do not have enough residence time in the stomach (Fig 1.b). As a result, frequency of dose administration in such cases have to be increased.[25]

Targeted delivery to increase the retention time of drugs in the specific absorption sites of the GI tract has received a great deal of attention within the last decade. Dosage forms that can be maintained in the stomach are called gastro retentive drug-delivery systems (GRDDS).[25] The gastroenteric delivery systems provide a uniform concentration/amount of the drug at the absorption site and thus during the absorption state, allow the maintenance of plasma concentrations within a therapeutic range, which minimizes side effects and reduces the frequency of administration. Moreover, gastroenteric delivery systems provide

potential for delivering new therapeutics under development such as large molecules including peptides, proteins, oligonucleotides, and vaccines.

These products provide numerous benefits compared with immediate release drugs, including larger effectiveness in the treatment of chronic conditions, reduced side effects, greater convenience, and higher levels of patient compliance due to a simplified dosing schedule. These systems can improve the controlled delivery of drugs that have an absorption window by continuously releasing the drug for a prolonged period before it reaches its absorption site thus ensuring its optimal bioavailability.[26]

Over the past three decades, the pursuit and exploration of new approaches have advanced consistently in terms of technology and diversity. A number of systems such as floating systems, raft systems, expanding systems, swelling systems, bio adhesive systems and low-density systems (Fig 1.c) have been developed.[26]

Typical carriers for therapeutics are natural polymers, including cellulose, chitosan, hyaluronic acid, alginate, dextran and starch, as well as on proteins, such as collagen, gelatin, elastin, albumin and silk fibroin.[27] The use of natural polymers remains attractive primarily because they resemble biological macromolecules, are often biocompatible or even biodegradable, are relatively inexpensive, and permit a variety of chemical modifications or functionalizations.[28]

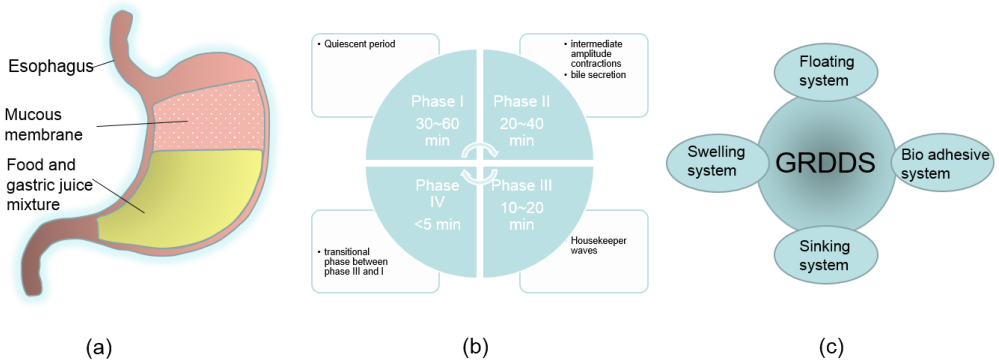

Figure 1. The human stomach and designs of gastroretentive drug delivery systems. Physiology of stomach: (a). Esophagus is a tube-like organ that connects the mouth and throat to the stomach. Small intestine (small bowel) is a long tube-like organ that extends from the stomach to the colon (large intestine or large bowel). The mucosa (mucous membrane) is the inner lining of the stomach. It has many glands that produce mucus, hydrochloric acid and digestive enzymes; 90~120 minute rapid interdigestive motility pattern of the stomach which consist of four phases (b); Classification of gastroretentive drug delivery systems (GRDDS) (c). Floating systems: low-density systems that can prolong the gastric retention time and increase bioavailability by floating on top of the gastric contents; Bioadhesive/mucoadhesive systems: a dosage form that can stick to the mucosal surface by different mechanisms; Swelling systems: Expandable drug delivery systems are small for easy swallowing and expand to a larger size after contact with gastric juices, which can prolong the gastric retention time; Sinking system: sinking system include materials that can sank to the bottom of the stomach and increase gastric retention time.

1.4. Silk based gastroretentive drug delivery systems

1.4.1. Introduction: reviews of molecular and physical properties of silk fibroin

Silk fibroin, a naturally occurring protein polymer, has several unique properties making it a favorable matrix for the incorporation and delivery of a range of therapeutic agents. Silk fibroin is biocompatible, slowly biodegradable, and equipped with excellent mechanical properties and processability. For illustration, here is a quick review concentrating on the molecular and physical properties of silk which affect drug release kinetics.[29]

1.4.2. Physical properties of silk fibroins

Silkworm fibroin consists of two structural proteins, the light chain (~25 kDa) and the heavy chain (~390 kDa). The structural protein gives silk its mechanical strength, softness, and elasticity.[30] Glue-like proteins named sericins which constitutes 25-30% of the silk proteins in cocoons (20 kDa to 310 kDa) hold the protein chains together in natural silk status.[29] Sericins have been recognized as the main source of immune responses, but due to their high hydrophilicity can be easily removed by boiling silk in alkaline solutions (Figure 3).[30]

The complete sequence of the *B. mori* silk fibroin gene has been well studied.[31] Detailed study shows the heavy chain of silk fibroin is composed of hydrophobic and hydrophilic blocks, where the hydrophobic blocks consist of highly conserved sequence repeats of GAGAGS hexamer and less conserved repeats of GAGAGV or GAGAGY that

make up the crystalline regions of silk fibroin by folding into intermolecular beta-sheets (Fig 2). Compared to the size of the hydrophobic regions, the hydrophilic part of the fibroin is non-repetitive and very short.[32] Polymer molecular weight strongly influences its mechanical properties and biodegradability, and, therefore, its qualification for drug delivery. Prolonging the boiling time of silk cocoons in Na_2CO_3 solutions causes hydrolytic degradation of the silk fibroin protein.[7] Enzymatic degradation or genetic engineering could also be methods to control the molecular weight of silk fibroin.[33] Although lower molecular weights may have compromised mechanical properties, that there exist variations in the processing of silk fibroin that can produce different molecular weights, which may influence bulk viscosity, bulk crystallinity, degradation rates and, thereby, the release kinetics of embedded drugs.[1]

Three main secondary structures, termed silk I, II and III, have been reported in silk fibroin. Silk I refers to the water-soluble structure existing within the silkworm gland before spinning. Silk II stands for the insoluble, more stable extended beta-sheet conformation which forms after the spinning of silk fibers from the spinneret of the silkworm. Silk III is an unstable structure observed at the water-air interface.[34] The hydrophobic blocks of silk fibroin make up the crystalline regions by forming crystalline intermolecular beta-sheets. The crystallinity of silk fibroin is the primary factor that influences its stability. A change in crystallinity influences the degradation rate of silk fibroin. Different treatments dehydrate and destabilize the random coil and/or the unstable silk I state of silk fibroin, leading to silk II (predominant) conformation, which characterized by an increase in beta-sheet content. The most common method to enrich silk fibroin in beta-sheet structure and

thus induce water insolubility is a treatment with methanol.[35] Additionally, high temperatures,[36] pH close to the isoelectric point of silk fibroin (which is about 4.0), the use of salts[37] and shear-force[38] were reported to increase its beta-sheet content. Additionally, genetic inclusion of elastin-like domains in silk fibroin could result in less crystallinity.[39] Alterations in both crystallinity and hydrophobicity offer options to influence the interaction between drug molecules and Silk fibroin. Moreover, a change in crystallinity influences the degradation rate of silk fibroin, which could be an attractive approach towards drug delivery systems with distinct release kinetics.

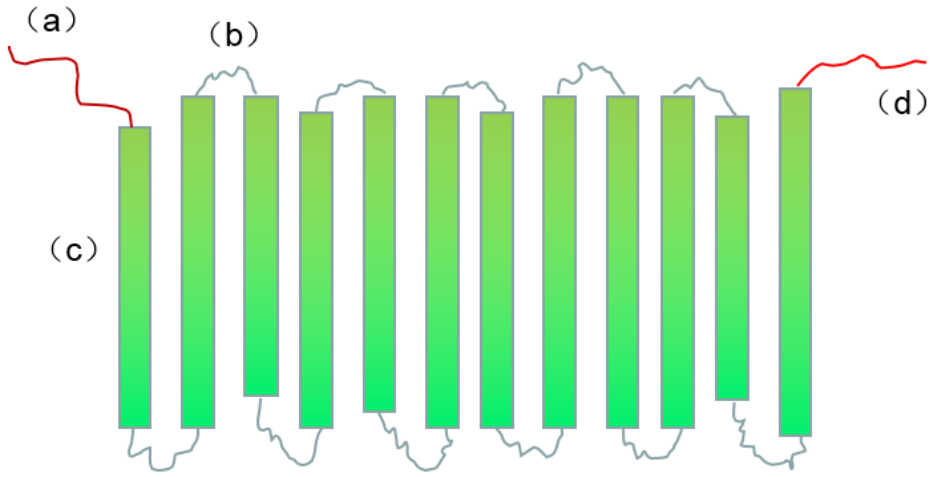

Figure 2. Schematic of silk fibroin heavy chain. N-terminal region (a), 12 repeating hydrophobic regions (bulk domains) (c), 11 charged linkages (b), and a C-terminal region (d) are labelled. The N-terminus, C-terminus, and 11 spacer regions are hydrophilic and form the less crystalline regions of the assembled proteins, and the 12 large bulk domains are hydrophobic and form the dominating crystalline beta-sheet regions that generate the physical crosslinks during the formation of hydrogels. Each hydrophobic crystalline region that is connected via the 11 nearly identical spacers is composed of 3 dipeptide units in form of Glysine-X (GX), where X can be alanine (A), serine (S), tyrosine (Y), valine (V), or threonine (T). Within these bulk hydrophobic domains, the hexapeptides GAGAGS are present in 433 copies and GAGAGY in 120 copies, accounting for 72% of the repeat domains. These regions form the physically cross-linked crystals or beta-sheets, resulting in the strength and stability of silk materials.

Crystalline silk fibroin is insoluble in water. Highly concentrated salt solutions of lithium bromide, lithium thiocyanate, calcium thiocyanate or calcium chloride are commonly applied to dissolve silk fibroin.[29] Such electrolyte solutions are able to disrupt the hydrogen bonds that stabilize beta-sheets. After solubilization, dialysis against water or buffers is performed to remove the electrolytes. The resulting aqueous silk fibroin solutions offer gentle processing conditions to fabricate drug delivery systems (Fig 3).

The stability of a polymer is an important feature for the storage of a drug delivery systems. Aggregation, gelation and of silk fibroin aqueous solution during storage has been observed. The untreated silk fibroin solution, although low in beta-sheet content, keeps its hygroscopic feature thus highly sensitive to humidity. High humidity incubation has been shown to contribute to beta-sheet transition of silk fibroin. However, systematic investigations on the storage stability of silk fibroin matrices are still under study.[40]

Silk fibroin displays exceptional thermal stability. The temperature Tg of proteins is considered to be a major determinant of protein self-assembly. Dry silk fibroin films demonstrated a Tg of approximately 175 ^{0}C.[41] The Tg of frozen silk fibroin solution was reported to be in the range of from -34 to -20 ^{0}C.[42] The higher the pre-freezing temperature above the glass transition, the longer time needed for ice crystals to form and grow in size.

The biodegradation rate of a drug delivery system for tissue regeneration should be adjustable to kinetically match the evolving environment during healing and regeneration. The degradation of many commonly used polymers in drug delivery is fast,[43] typically in the range of days or weeks even years for example many poly(lactid*e*-co-glycolide) (PLGA)

copolymers. However, the hydrolytic degradation of silk fibroin has been shown to be slow. In fact, it was demonstrated that the hydrolytic degradation of water vapor treated Silk fibroin scaffolds in *vitro* is minor, with only about 4% mass loss within 7 weeks.[15] Being a protein, biodegradation of silk fibroin predominantly occurs through proteolytic enzymes, and, has been described directly influenced by its beta-sheet ratio.[44]

1.4.3. Biocompatibility of silk

Unlike commonly used polymers such as poly(lactide) and collagen in drug delivery research, silk has fewer inflammatory symptoms and foreign body responses.[45] For instance, in *vitro* research has shown that silk is biocompatible with osteoblast cells[46] and hippocampus neurons.[47] A further one year implantation study in rats demonstrated that both aqueous- and HFIP-derived scaffolds were well tolerated by the host animals, and the host immune response to the implanted scaffolds was low and local.[45]

1.5. Silk hydrogel for drug delivery

1.5.1. Introduction: advantages of silk proteins as biomaterials for drug delivery

A desirable drug delivery system should release the drug in a slow, sustained manner. Silk protein is part of these candidates which not only fits the need but are also biocompatible, biodegradable, mechanically durable and can be prepared and processed under ambient aqueous conditions to avoid loss of drug bioactivity.[48]

Comprehensive studies have demonstrated that silk is less inflammatory and therefore more biocompatible than commonly used biodegradable polymers include poly(lactide) and collagen.[49] This feature makes the use of silk, specifically in biomaterial formats for tissue drug delivery, advantageous when compared with most other natural or synthetic polymers. Moreover, due to the beta-sheet formation, silks exhibit relatively slow degradation both in *vitro* and in vivo.[50] The biodegradation rate can also be adjusted by controlling the degree of beta-sheet content via different processing methods.[50] Many chemical modifications could be applied to silk fibroin. It is also estimated that by introducing functional groups to the fibroin, a variety of drugs in different amounts can be loaded and released with distinct kinetics. Nevertheless, local silk fibroin functionalization can also promote cell adhesion or address cellular signaling pathways through specific cell-matrix interactions.

Importantly, silk fibroin is versatile in terms of processability and has been successfully formed into various silk protein-based drug or gene delivery systems by using biologically relevant conditions of water, ambient temperature, and physiologically

relevant chemicals (Fig 3). Silk-based drug delivery designs include hydrogels,[51] silk-coated solid reservoirs,[52] microspheres,[53] nanofilms/layer-by-layer coatings[54] and specific interactions/surface decorations.

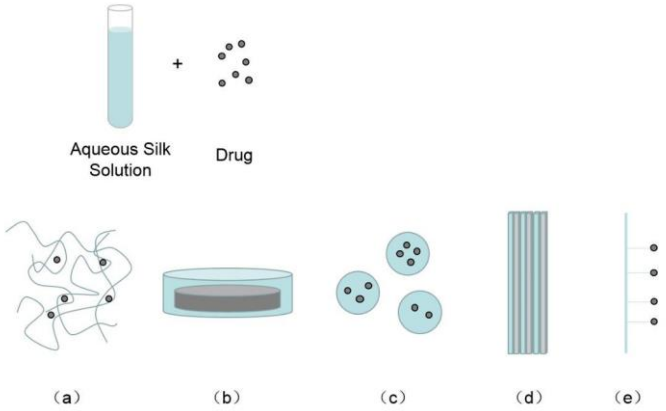

Fig 3. Various silk protein-based drug or gene delivery systems

(a): Hydrogels; (b): Silk-coated solid reservoirs; (c): Microspheres; (d): Nanofilms/layer-by-layer coatings; (e) Specific interactions/surface decoration.

1.5.2. Current silk hydrogel drug delivery systems and limitations

Among these different drug release carriers, silk hydrogels were selected as my current research target. Their highly porous structure can easily be tuned by controlling the density of crosslinks in the gel matrix. The porosity also permits loading of drugs into the gel matrix and subsequent drug release at a rate dependent on the diffusion coefficient of the small molecule or macromolecule through the gel network. Hydrogels are also relatively deformable and can conform to the shape of the surface to which they are applied. The mucous-adhesive or bio-adhesive properties of some hydrogels can be advantageous in immobilization them at the site of application which is the gastric mucus surface.

Despite these many advantageous properties, silk hydrogels are given one main limitation. The traditional processed silk hydrogel can resist enzyme digestion and degrade slowly (days to months) both in *vitro* and *vivo* compared to gastrointestinal digestion time (<16h).[45] Thus, the drug loaded cannot completely release to target gastric surface. As a result, part of the loaded drug may be released in intestine or other parts of the body which is undesired in stomach specific drug delivery study.

1.5.3. Silk electrogelation-novel gelation method for silk drug delivery approach

Silk fibroin, as a hydrophilic−hydrophobic−hydrophilic polymer, was confirmed to form micelle structures of 10~100 nanometers in water in which the terminal hydrophilic blocks consist of the outer surface of the micelles, while the hydrophobic blocks and small hydrophilic blocks are detected inside the micelles.[31b]

In previous studies, the hydrophobic and hydrophilic blocks of silk fibroin were assumed to be randomly distributed after silk regeneration. The hydrophobic blocks then gradually arrange to from small nanoparticles via electrostatic repulsion, while the hydrophilic blocks move to the surface of nanoparticles to interact with water.[31b] With the induction of time, high temperature, vortexing, chemical or enzymes, the metastable silk I structure of silk (organized but not beta sheet) could transfers into the stable silk II (beta sheet) structure to from a silk hydrogel. Once the hydrogel formed, it cannot return to solution state.[47]

Recently, a novel approach using electro fields to from silk electro hydrogels (*e*-gel) has been reported.[8] under the presence of low-voltage direct-current (DC), the proton concentration increases in the vicinity of the positive electrodes, resulting in a reduction of local pH and reduce the repulsive forces of the negatively charged amino acid groups which in neutral aqueous solution, were considered as the main force to prevent intermolecular self-assembly to form micelles. The micelles of silk then aggregated to larger globules following the shielding of the repulsive negative forces. Unlike normal hydrogels, silk electrogels (*e*-gel) have several unique characteristics such as reversibility and adhesiveness which make it an appropriate candidate for drug delivery applications.[8]

1.5.4. *E*-gel morphological features

Further FTIR study indicated intermediate structures play an important part in electrogelation since *e*-gel formation results in a significant increase in alpha-helix and a notable decrease in random coil content, rather than beta-sheet formation as in normal sol-gel transition process.[55] Corresponding DSC shows a decrease of the crystal peak after electro-gelation, which suggests the appearance of intermediate structures in low voltage DC-directed gelation as well.

Morphological features of silk *e*-gel assessed by SEM image revealed the presence of freezing artifacts, including distortions in pore size and shape, and cracks on the surface. Additional chemical crosslinking preserved silk fibril micromorphology after freeze-drying. A closer look at lyophilized silk *e*-gel shows spherical, micelle and micrometer scale structure from several tens of nanometers to several micrometers. The larger microspheres with diameter of micrometers were assembled from the small microspheres with diameters of several hundred or several tens of nanometers. The results suggest the *e*-gel was assembled from nanoparticles with sizes of about 10 nm under an electric field then self-assembled to larger microspheres.

1.5.5. *E*-gel reversibility and stability

Crystalline silk fibroin is insoluble in most solvents. However, the *e*-gel system is a reversible material system which can return to the solution state in a high pH solution or by applying reverse voltage. On the other hand, the *e*-gel system displays stability in low pH solution. (pH point<=4). This acid stable feature is due to silk fibrin's pI. (pI=4.2) The amazing pH-sensitive reversibility of *e*-gel system gives *e*-gel system potential as a pH-specific, short-term release drug delivery system.

In summary, the interesting characteristics of alpha-helix rich silk *e*-gel include adhesive properties and reversibility of higher pH, which raise possibilities for the development of a mucus adhesive, gastric specific and short-term release drug delivery system.

1.6. Statement of purpose

The gelation process includes the formation of inter- and intramolecular interactions among the fibroin protein chains (including hydrophobic interactions and hydrogen bonds) and the fibroin chain interactions (input of energy into the solution, reducing repulsion among the chains or dehydration to remove the water molecules that stabilize the hydrophobic moieties in solution). These physically cross-linked, beta-sheet rich hydrogels are considered long term biodegradable materials and have been applied to a wide range of drug delivery applications. The degradation mode in vivo is influenced by the beta-sheet content. In some cases, such as gastric drug delivery applications, the short term, controllable drug delivery is desirable. Thus it is important to study the recently developed, alpha helix rich, short time reversible electro gel system which formed through a weak electric field to gain a full picture of silk e-gel as a gastric drug delivery system.

Since *e*-gel is relatively short duration in solution, chemical modification of silk e-gel to extend its release profile is required. In the present work, we hypothesized that the degradation behavior of silk electro hydrogel in gastric juice could be influenced by the introduction of beta sheet during gelation. We used glycerol to induce beta sheets in silk electro gels and used doxorubicin to evaluate the usefulness of silk fibroin hydrogels for oral gastric drug delivery applications. The structural transition was analyzed via experiments such as FTIR, DSC and TGA. Doxorubicin is used as a model drug to treat many kinds of cancers including leukemia, breast cancer, bone cancer, lung cancer, and brain cancer. Understanding how doxorubicin loading and release would be helpful for the development of cancer treatment based on e-gel. It is hoped that these techniques will allow

us to first establish an understanding about the structural transition of silk electro gel mixed with glycerol and the potential of this system as a drug delivery system in gastric juice. Information relating to cell toxicity, drug release efficiency against cells will be pursued, thus providing new approaches to a well-developed silk based short term drug release system.

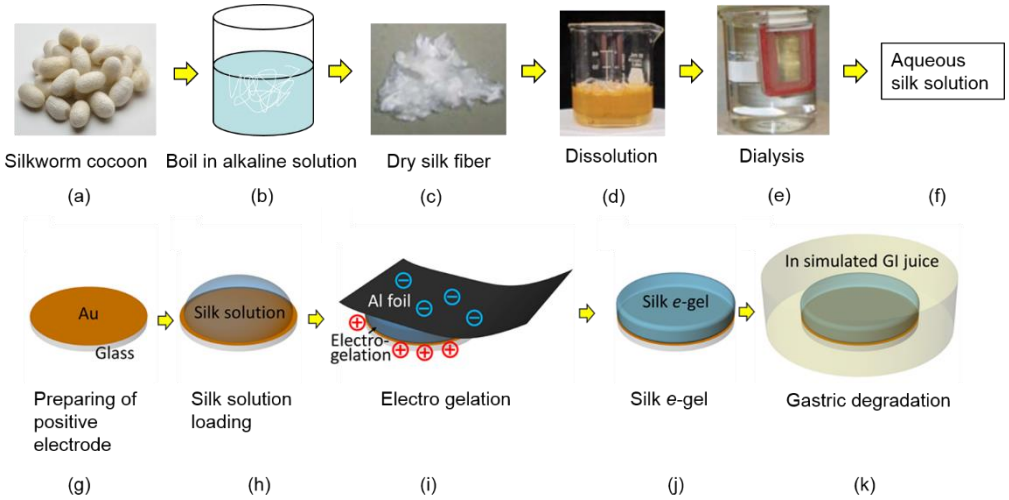

Figure 4. Overview of the whole electro-gelation and gastric degradation process. Sericin is removed from silk by boiling *Bombyx mori* cocoons in an alkaline solution (a, b). Dry and degummed silk fibroin is dissolved in salt (c, d). The aqueous silk solution without salt can be achieved via dialysis (e, f). The positive electrode is made by coating gold on the surface of coverslips (g). two hundred uL 3% w/w% silk solution is pipetted on the surface of gold coated coverslips (h). During the electrogelation process, the gelation proceeded on the surface of the positive electrode (i). After gelation the negative electrode is removed (j). The silk e-gel is moved to gastric juice for further degradation process (k).

CHAPTER 2

MATERIALS AND METHODS

In this study, silk electro gel was chosen due to its potential for short term drug delivery in the gastric juice. Beta sheets help extend acid stability was induced via glycerol and characterized. To further understand the potential of silk *e*-gel as a cancer treating drug delivery vehicle, experiments were established to evaluate the loading and release profile of doxorubicin in *vitro*. Finally, cell toxicity experiments provide insight to the bio application of the hydrogel.

2.1. Preparation of aqueous silk fibroin solutions

Silk fibroin aqueous solutions were prepared as previously described.[56] Briefly, *B. mori* cocoons (Sumiyoshicho, Naka-ku,Yokohama, Japan) were boiled for 10 min in an aqueous solution of 0.02 M sodium carbonate (Na_2CO_3, 99%, Sigma-Aldrich) and then rinsed thoroughly with deionized water. After overnight drying the silk fibroin was dissolved in an aqueous solution containing 9.3 M lithium bromide (LiBr, 99%, Sigma-Aldrich) at 60 0C for 4 hours to break down the inter-chain hydrogen bonds existing in the beta-sheets structure and return it to the alpha-helix predominant water-soluble form. The solution was dialyzed against deionized water using Slide-a-Lyzer dialysis cassettes (Pierce, molecular weight cut-off 3,500 Da) for 72 hours to remove the salt. The solution was optically clear after dialysis and was centrifuged at 8,700 RPM for 20 minutes twice to remove small amounts of aggregates that formed during the process.

The final concentration of aqueous silk fibroin solution was 3 wt.%, determined by weighing the remaining solid after drying. The fresh silk fibroin solution was stored at 4 0C for 1 week for aging.

2.2. Electrogelation of silk fibroin solutions

One week aged regenerated silk solution (3 wt %) was prepared. 50% glycerol (water: glycerol 1:1) mixed silk solution (total volume 200 uL) at three different ratios (silk: 50% glycerol at ratio 3:1; 2:1; 1:1) were held between positive electrodes (gold coated coverslips with a diameter of 12 mm) and negative electrodes (aluminum foil) to from *e*-gels.[8] The electrochemical growth of the silk hydrogel was induced at the solution/positive electrode interface by applying a constant voltage of 15 V across the parallel electrodes using a DC power supply (Agilent E3612A DC power supply, Agilent Technologies, Inc., Englewood, CO). During a 30s gelation process, a visible gel formed at the positive gold electrode as indicated in Figure 5.

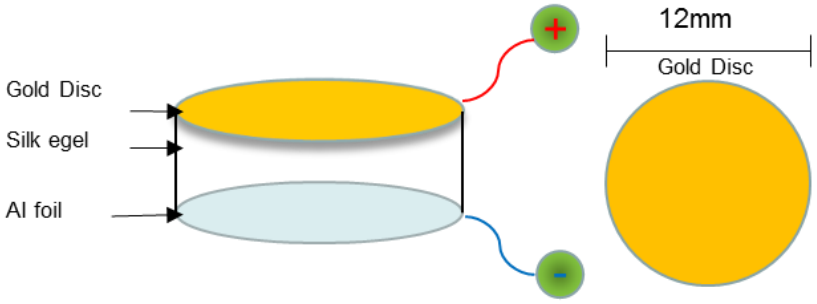

Fig 5. Schematic diagram of the experimental Setup for the electrogelation of the regenerated silk. The 200 µL, 3 wt% silk solution was added between two electrodes (Diameter: 12 nm). A 15 V DC electric potential across the parallel electrodes induced the formation of electro-gelation on the positive side. Over 30s the gel forms around the positive electrode.

2.3. Fourier transform infrared spectroscopy (FTIR)

The structural changes in the silk solution and gel states were analyzed using a JASCO FTIR 6200 spectrometer (JASCO, Tokyo, Japan) equipped with a MIRacle™ attenuated total reflection [8]. Ge crystal cell in reflection mode. All samples were flash frozen and lyophilized to preserve the structure of silk *e*-gel. Background measurements were taken with an empty cell for freeze-dried samples or from deionized water in the case of hydrated samples and the data were subtracted from the sample readings. For each measurement, 128 scans were coded at a resolution of 4 cm^{-1}, with the wavenumber ranging from 400 to 4000 cm^{-1}. Fourier self-deconvolution (FSD) of the infrared spectra covering the amide I region (1595^{-1}~705 cm^{-1}) was performed using Opus 5.0 software to identify silk secondary structures. Deconvolution was performed using a Lorentzian line shape with a half-bandwidth of 25 cm^{-1} and a noise reduction factor of 0.3. FSD spectra were curve fitted to measure the relative areas of the amide I region components.[57]

2.4. Differential scanning calorimetry (DSC)

The flash frozen and lyophilized samples of silk *e*-gel were encapsulated in aluminum pans and heated in a TA Instruments Q100 DSC (New Castle, DE) with a dry nitrogen gas flow of 50 mL/min. The instrument was calibrated for an empty cell baseline and with respect to an indium standard for heat flow and temperature. The samples were heated at 3 $^{o}C\ min^{-1}$ from -50 to 250 ^{o}C with a modulation period of 60 s and temperature amplitude of 0.318 ^{o}C. The data were recorded with TA instrument's Q series explorer software. The analyses of the data was done with TA Instrument's Universal Analysis 2000 software.[57]

2.5. Thermal behavior measurement (TGA)

Silk *e*-gel samples were lyophilized overnight after electro-gelation and frozen at -20 ^{o}C before use. All the samples were cut into 4 mg separately and loaded in platinum crucibles. The thermogravimetric analysis was then performed using a TA instruments, SDT Q600 (Luken's drive, New Castle, DE). The samples were non-isothemal heated from RT (22 ^{o}C) to 600 ^{o}C at a heating rate of 3 ^{o}C min^{-1}. The TGA was carried out in nitrogen with the flow rate of 50 mL/min. The data was recorded with TA instrument's Q series explorer software. The analyses of the data were done with TA Instrument's Universal Analysis 2000 software.[58]

2.6. Silk *e*-gel in *vitro* acidic degradation

The in *vitro* experiments of silk *e*-gel acid dissolution used acid buffer and artificial gastric juice (Pepsin, CAS# 9001-75-6, <1% w/v, Lactic Acid, CAS# 50-21-5, <1% w/v, Hydrochloric Acid, CAS# 7647-01-0, <1% w/v, Water, purified, CAS# 7732-18-5, >99% w/v, Fisher Science Education) as the medium. To mimic stomach gastric dissolvation, the silk hydrogel and silk/glycerol mixed hydrogel after electro-gelation (200 μL solution/30s gelation time) were immersed in 3 ml of artificial gastric juice at 37 ^{o}C. A 25 μL of the solution was taken and replaced with the same volume of fresh gastric juice at every 15 minutes till the end of the four hours.

To further investigate the protein release curve in longtime storage, silk electro-hydrogels were immersed in 3 ml of acidic buffer (pH=2, 1M acetate acid: sodium acetate)

for 2 weeks. 25 μL of the solution was replaced with flash buffer every day to monitor protein release from the silk *e*-gel.

The concentration of silk protein at different time points was detected through the BCA assay. Each 25 μL of the solution was added to 250 μL of the BCA reagent and incubated at 37 °C for half an hour. The absorbance was read using plate reader (SpectraMax M3; Molecular Devices, Sunnyvale, CA) at 595 nm. The protein concerntain was then calculated using a standard curve.

2.7. Silk *e*-gel in *vitro* drug loading

The doxorubicin loaded silk *e*-gels were prepared through the electrogelation of doxorubicin (D-4000 Doxorubicin, Hydrochloride Salt, LC laborites) mixed silk solution (final doxorubicin concentration of 0.1mg/mL).[59] Silk *e*-gel, silk/glycerol mixed *e*-gel was prepared separately on the surface of gold coated coverslips. After gelation, silk *e*-gels were removed from gold coated coverslips and dissolved in 250ul 9.3 M LiBr at 60 °C for 5 minutes. Solutions were then mixed with 750 μL PBS (Sigma-Aldrich) immediately. The fluorescence intensity was detected with a plate reader (SpectraMax M3; Molecular Devices, Sunnyvale, CA) and compared with a standard curve. The loading ratio (%) was determined based on the 100% release of doxorubicin from the silk *e*-gel.

$$\text{encapsulation efficiency (w/w\%)} = \frac{\text{amount of model drug in particles}}{\text{model drug initially added}} \times 100$$

2.8. Silk *e*-gel in *vitro* drug release

The doxorubicin loaded silk e-gels were prepared as previously described. After gelation, silk e-gel, silk/glycerol mixed e-gels were immersed in 5 ml of artificial gastric juice at 37 oC for up to 4 hours. The 100 μL of the solution was taken and replaced with the same volume of fresh gastric juice at every 15 minutes till the end of four hours.

The release behavior of doxorubicin was characterized at excitation wavelength 445nm and emission wavelength 595nm. Fluorescence intensity at each time point was measured by a plate reader (SpectraMax M3; Molecular Devices, Sunnyvale, CA). The silk e-gel without doxorubicin loading was used for background calibration. Cumulative release (%) was identified based on the 100% release of doxorubicin from the silk.

2.9. Cell culture of human gastric cancer cells

The human gastric cancer cell line NCl-N87 (ATCC CRL-5822) was obtained from the American Type Culture Collection (ATCC) and maintained in RPMI 1640 cell culture medium (ATCC) containing 10% fetal bovine serum (Life Technologies Inc) and 10% penicillin and streptomycin (Life Technologies Inc.). The medium was changed every other day.[60]

2.10. In *vitro* cytotoxicity and drug release

The in vitro cytotoxicity and drug release test was assessed with a AlamarBlue Assay (AlamarBlue® Cell Viability Assay Kit purchased from Life Technologies Inc) against NCL-N87 (N87) cells.[61] For cell viability, N87 cells were seeded on transwells (Corning®

HTS Transwell®-24 well permeable supports HTS Transwell-24 units W/ 0.4 μm pore polycarbonate membrane and 6.5mm inserts) in 24 well plates（Corning® Costar® Cell culture plates）are combined at the concentration of 10,000 cells per well with 1000 μL RPMI medium. N87 cells were incubated for 7 days to generate a gastric epithelial surface. Medium was changed every 2 days to maintain cell's the epithelial phenotype. After one week incubation with PBS, silk *e*-gel (200 ul volume before gelation) and silk/glycerol mixed *e*-gels (200 ul volume before gelation) were added to each well separately. The cells were subjected to AlamarBlue Assay after being incubated for another 6h, 12h, 24h or 48h. At each checkpoint of the experiment, the culture medium was replaced by 1000 ul AlamarBlue assay solution (alamar blue solution: RPMI at ratio 1:9). The plate was subsequently returned to the incubator. After 2.5 hour incubation, each 100 μL AlamarBlue assay solution was carefully removed from the plate and read by the plate reader (SpectraMax M3; Molecular Devices, Sunnyvale, CA). Fluoresce signal of the solution was measured at excitation wavelengths 550nm and emission wavelengths 590nm. Cell viability (%) was measured by (sample/control) x 100, where sample and control stand for the fluoresce signal of each well.

2.11. In *vitro* cellular uptake of doxorubicin

Cellular uptake experiments were performed using fluoresce microscopy. NCI-N87 cells (ATCC CRL 5822, human gastric carcinoma) were cultured in 24-well cell-culture plates（Corning）in RPMI-1640 Medium (ATCC® 30-2001™) supplemented with 10% FBS (Gibco) and 1% Penicillin/Streptomycin at 37 ℃ in 5% CO2 at the concentration of

15,000 cells/cm^2 for 7-10 days to ensure cell attachment, proliferation and gastric morphology transition. The medium was changed every other days to maintain the epithelial phenotype of NCI-N87 cells. After the cells formed a integrate epithelium, they were treated with free doxorubicin (200 μL, 100 μL/ml), doxorubicin loaded silk e-gel, and doxorubicin loaded silk/glycerol e-gel separately for 1h. After incubation period, the cells were washed three times with PBS and fixed with 4% paraformaldehyde for 15 min at room temperature. The cell nuclei were stained with DAPI (Invitrogen), following the manufacturer's instructions. The doxorubicin uptake was visualized through The CLSM images were obtained on OLYMF'US IX81 (OLYMF).[62]

2.12. In *vitro* drug release and morphological analysis

In vitro drug release experiments and morphological analysis was assessed with SEM with NCL-N87 cells. One week incubated NCL-N87 cells (10,000 cells per transwell) were cocultured with free doxorubicin (100 μg/ml, 200 μL), doxorubicin loaded silk *e*-gel, and doxorubicin loaded silk/glycerol *e*-gel for up to 2 days. Time zero incubated and 48h incubated samples were collected and taken through critical point drying. The cells were cross-linked with 1% glutaraldehyde for 4h, and progressively dehydrated in a graded series of ethanol (30%, 50%, 75%, 95% and twice in 100%, 30 min at each concentration). The samples were subsequently dried by critical point drying with a liquid CO2 dryer (AutoSamdri-815, Tousimis Research Corp., Rockville, MD). Then Morphological analysis of the electrogels were conducted using an scanning electron microscope (Zeiss UltraPlus SEM or Zeiss Supra 55 VP SEM, Carl Zeiss SMT Inc., Peabody, MA) at a voltage

of 2−3 kV after Pt/Pd coating using a sputter coater (208HR, Cressington Scientific Instruments Inc., Cranberry Twp, PA).[63]

CHAPTER 3

RESULTS

3.1. Structural changes in the electrogelation process

Structural changes after electro gelation and subsequent glycerol mixed silk *e*-gels were studied by FTIR, DSC and TGA assays (Fig. 6, 7, 8 and 9). Fourier Transform Infrared Spectroscopy (FTIR) had been used to provide information on the secondary structure of polypeptide and proteins since 1950s.[64] The amide I (1600~1700 cm^{-1}) and amide II (1480~1575 cm^{-1}) vibrations were sensitive to the secondary structure of the backbone. The FTIR spectral region between 1600 and 1700 cm^{-1} was commonly assigned to the absorption of the peptide backbone in secondary structures of silk fibroin since it had a more straightforward correlation with secondary structure. Table 1 listed the wavenumber ranges corresponding to vibrational bands in *B. mori* silk, within the amide I region of the spectrum, along with the literature references.

The amide I bands were deconvoluted to determine the fraction of the beta-sheets formed during crystallization using the method of Fourier self-deconvolution (FSD) over the amide I peaks on the spectra using Opus 5.0 software with Lorentzian peak profile (half-bandwidth of 25 cm^{-1} and a noise reduction factor of 0.3).[65] In this approach, the broad and typically indistinct amide I bands were transformed to yield a fitted self-deconvoluted set of bands from amide I′ (prime refers to the resultant spectrum), from which the secondary structural elements were determined.[66] The peak positions and assignments of the amide I region vibration bands of silk fibroin were determined by reference to the literature, and

listed in Table 1. Generally wavenumbers between 1620~1630 cm^{-1} were intimidated as intermolecular beta sheets, 1630~1667 cm^{-1} were belonging to random coils and alpha-helixes, and 1670~1695 cm^{-1} to turns. 1595 and 1615 cm^{-1} were belonging to side chains or aggregated strands.[64b, 67]

Table 1. Vibrational Band Assignments in the Amide I Region for *B. Mori* Silk Fibroin

Wavenumber Range (cm^{-1})	Peak Assignment	Reference
1605-1615	Side chains (Try)	[66]
1616-1621	Beta-strand/intermolecular Beta-sheet (weak)	[66]
1622-1627	Intermolecular beta-sheet (strong)	[66]
1628-1637	Intramolecular beta-sheet (strong)	[66]
1638-1646	Random coils/extend chains	[64b, 67]
1647-1655	Random coils	[64b, 67]
1656-1662	Alpha-helices	[64b, 67]
1663-1670	Turns	[66]
1671-1685	Turns	[66]
1686-1696	Turns	[66]
1697-1703	Beta-sheet (weak)	[64b, 67]

Peak positions and assignments of the amide I region vibration bands of silk block copolymer were determined by reference to the literature.

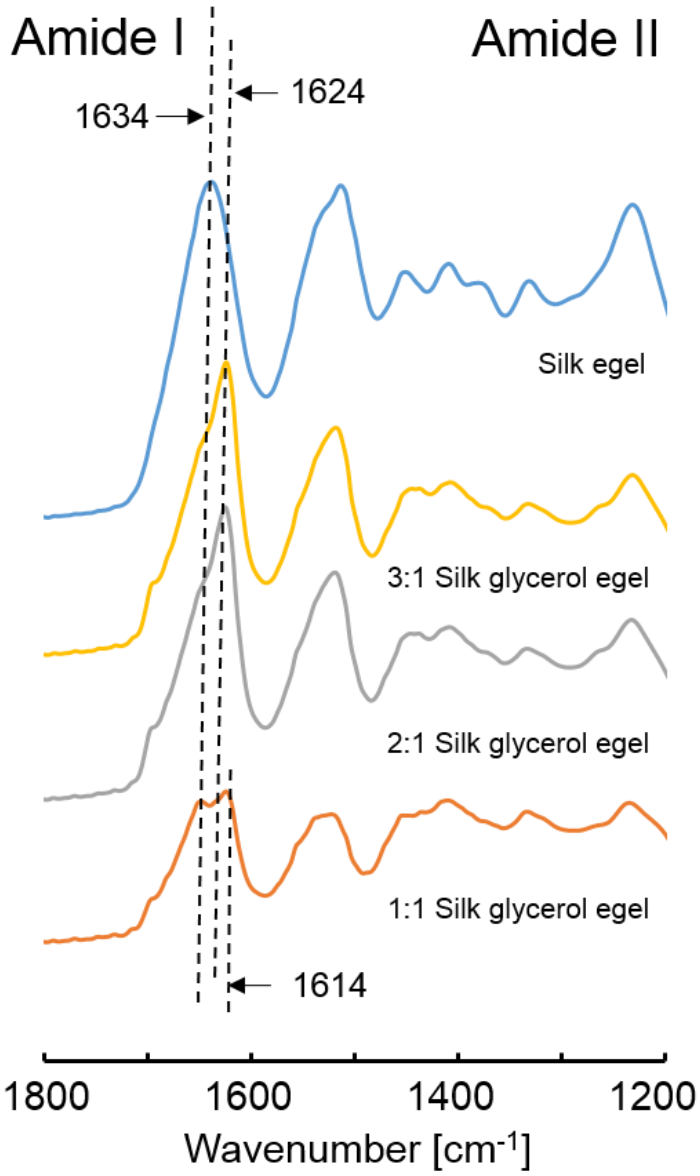

Fig 6. FTIR spectra of untreated, glycerol mixed silk *e*-gel at ratios 3:1, 2:1, 1:1. FTIR spectra of the freeze-dried electrogelled silk e-gels. The glycerol mixed silk *e*-gels (3:1; 2:1; 1:1) exhibited a shift from alpha-helix to beta-sheet compare to silk *e*-gel (3% wt%) after gelation. Notably, the beta sheet content decreased increase with the ratio of glycerol in all three glycerol treated samples (n = 3).

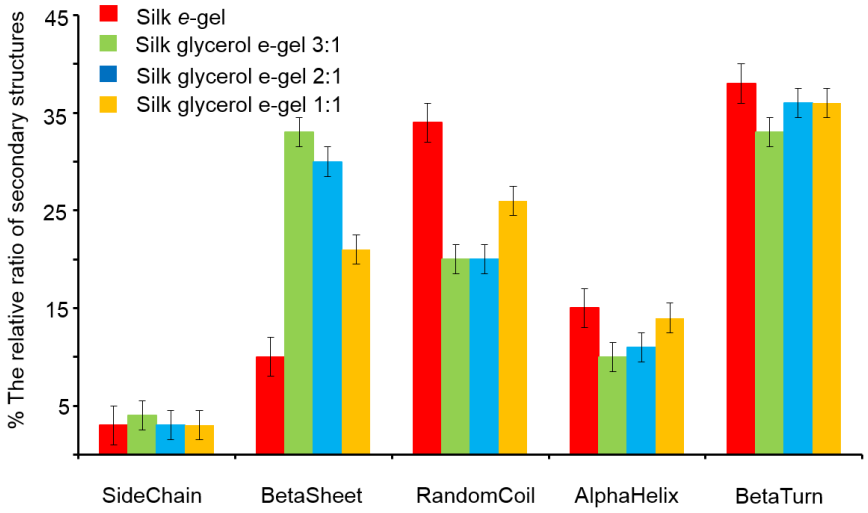

Figure 7. The relative ratio of secondary structures in silk e-gel and the silk glycerol mixed e-gels

(n = 3, error bar = standard deviation)**.**

The FTIR spectrum of silk *e*-gel and glycerol mixed silk *e*-gels of beta-sheets (1624 nm^{-1}), random coils/alpha-helices summed together (1634 nm^{-1}), and turns (1660 nm^{-1}) were shown in Figure 6. The ratios of the individual peak area to the total amide I band area were deconvoluted and shown in Figure 7.

Consisted with our previous studies about silk electro gel,[68] silk *e*-gel's amide I peak appeared at about 1635 cm^{-1} and 1660 nm^{-1} after e-gel formation, while no peak of specific beta-sheet absorption appeared. Silk *e*-gel had generally a random coil and beta turn structure (34% and 38% respectively) after electrogelation. We found, however, that as the ratio of glycerol increases in Figure 7, the side-chain fraction in amide I remained stable, the turn structure was also stable expect silk glycerol mixed *e*-gel in the ratio 3:1. On the other hand, we saw that with the addition of glycerol, glycerol mixed silk *e*-gel showed a significant peak transition from 1635 cm^{-1} to 1624 cm^{-1} (specific b-sheet absorption) after *e*-gel formation. Notably, the ratio of beta-sheet dropped as the ratio of glycerol arose. The initial ratio of beta sheet in pure silk e-gel was 10% after gelation, then rose to 33% after 12.5% w/w glycerol induction. A further increase glycerol ratio dropped the ratio of beta sheet significantly from 33% to 30% (2:1) and 21% (1:1) respectively.

In the heating process with DSC (Fig 8), the pure silk *e*-gel showed a significant crystallization endothermic peak between 210 ^{o}C and 220 ^{o}C. On the other hand, the glycerol mixed silk *e*-gels did not show any crystallization peaks. Another interesting thing that deserve notice is that all glycerol mixed silk *e*-gels had the melting peaks shifted from high temperature to a lower temperature.

The thermograms of silk *e*-gels were presented in Fig 9. The initial weight loss below 100 ℃ was considered water evaporation. Silk egel had a decomposition peak at about 260 ℃. Glycerol treated silk *e*-gels, which were shown to have more beta-sheet and amorphous structures than silk *e*-gel in FTIR and TGA assays, had significantly lower decomposition peaks than pure silk *e*-gel.

The ratio of glycerol also affected silk *e*-gel's thermostability. Glycerol mixed silk e-gel at ratio 1:1 showed higher decomposition temperature (205 ℃) in DSC curves than the lower ratio glycerol mixed egels (around 200 ℃).

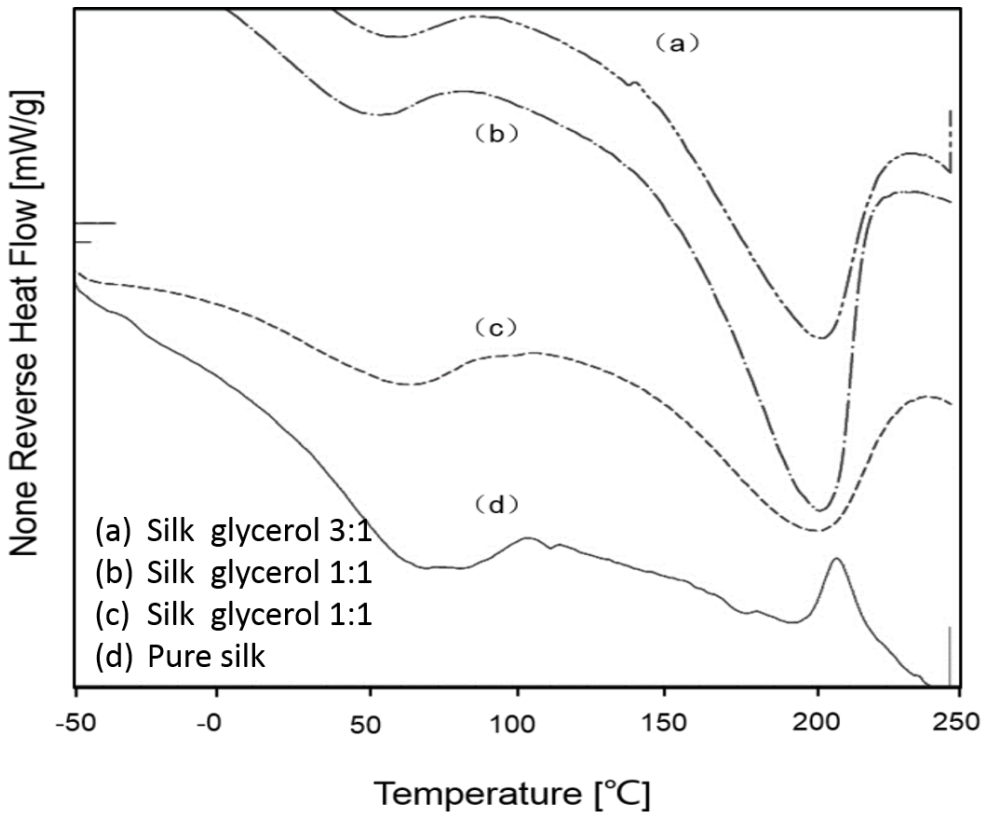

Fig 8. DSC scans collected from lyophilized samples of silk *e*-gel and silk glycerol mixed *e*-gels at ratio 3:1, 2:1, 1:1. (Region between 150 and 200 is magnified to highlight crystallization transitions). a) Glycerol mixed silk egel at ratio 1:1, b) glycerol mixed silk egel at ratio 2:1, c) glycerol mixed silk egel at ratio 3:1, d) 3 wt % silk e-gel (n = 3).

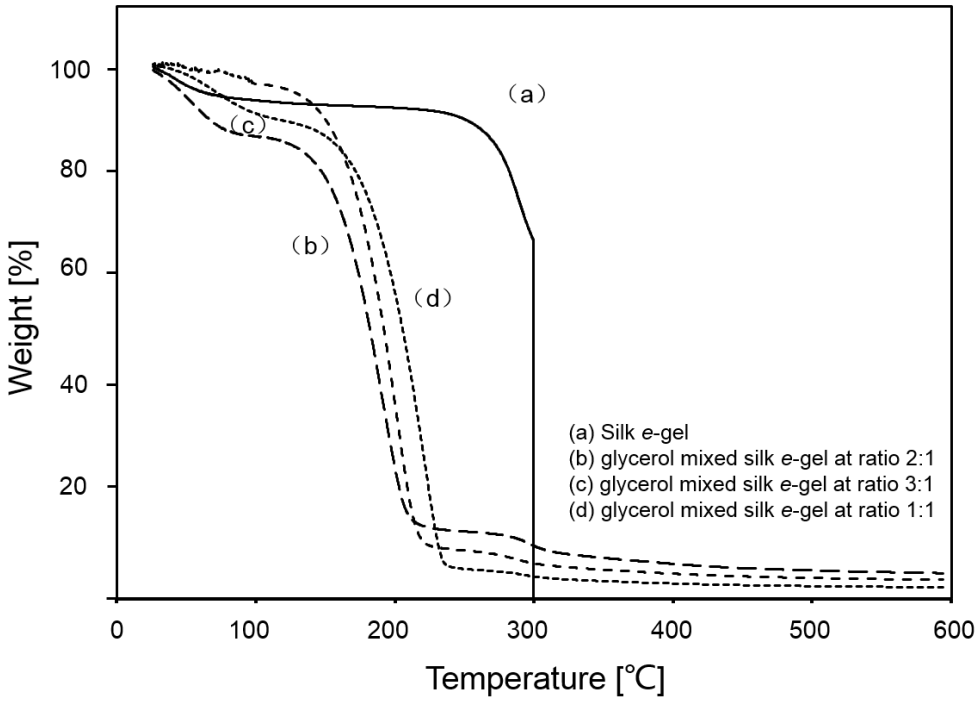

Figure 9. Thermograms assay of silk *e*-gel and silk glycerol mixed *e*-gels at ratio 3:1, 2:1, 1:1. Thermogravimetric curves of silk *e*-gels. Left hand axis: weight loss. X-axis: temperature. (a); glycerol mixed silk egel at ratio 3:1 (b); glycerol mixed silk egel at ratio 3:1 (c); glycerol mixed silk egel at ratio 3:1 (d)). The initial weight loss, below 100 °C, was due to water evaporation. Addition of glycerol content in the *e*-gel decreased the temperature of thermal degradation, indicating that glycerol impair *e*-gel's a thermal stability in the silk *e*-gels (n=3).

3.2. Silk *e*-gel in *vitro* gastric degradation

To determine the behavior of the silk electro hydrogels in the gastric juice, the dissolve curves of silk *e*-gel in gastric environments was studied (Fig 10). The volume of silk/silk glycerol solution (200μL), gelation time (30S), surface area of positive electrodes (113.04 mm^2) and voltage (15V) were set to ensure consistency during the electro gelation process. After gelation, silk *e*-gels as well as gold coverslips were incubated at 37 ℃ in 3 ml gastric juice. The original protein concentration level of gastric juice as well as the following silk *e*-gel released protein concentrations was detected through the BCA assay. Samples were collected every 15 minutes till the end of 4 hours. In gastric juice pure silk *e*-gels showed a burst release after 90 minutes of about 75%, followed by complete release after 180 minutes. In contrast, glycerol mixed, beta sheet rich *e*-gel as led to a retardation of the release of silk proteins. Within the same time period (90 minutes), only 54.2% (3:1), 56% (2:1) and 72.5% (1:1) of the silk protein were released from silk *e*-gel, respectively. The release of the glycerol mixed silk *e*-gel was continuous after 4 hours irrespective of the different ratios of glycerol.

.

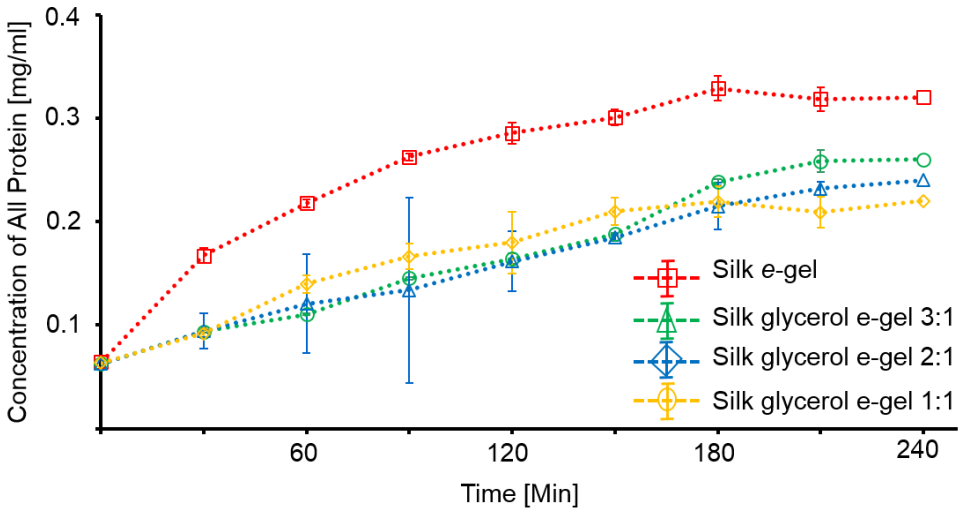

Fig 10. Cumulative release of silk protein in gastric juice. Silk was regenerated into 3% silk solution. *E*-gels were formed under the same condition (15V, 30s gelation time, 113.04 mm^2 surface area of positive electrode and 200μL solution volume). A cumulative 240 minutes silk protein release profile from silk egel, silk glycerol mixed *e*-gel at ratio 3:1, silk glycerol mixed *e*-gel at ratio 2:1 and silk glycerol mixed *e*-gel at ratio 1:1 was revealed via BCA assay. Data is expressed as concentration of proteins. 0.05 mg/ml protein concentration at 0 min stands for pepsin and other protein initially exist in artificial gastric juice (n = 3, error bar = standard deviation).

3.3. Silk *e*-gel *in vitro* stability

Silk e-gel, although stable in acid solution without pepsin for short term, can slowly dissolve in acid environment without pepsin in long run. To further investigate the stability of silk e-gel as a potential drug delivery system. The silk e-gels were made though the same process and store in a refrigerator at 4 ℃ and in 1 M pH 2 acetate acid buffers. The two week release profile was characterized through BCA assay. Data was collected every day at 9 PM.

The cumulative release profiles of all silk e-gels in Figure 11 showed samples remain considerably stable up to one week and only 4.5% (silk) ,20.1% (3:1), 28.6% (2:1) and 30.5%（1:1）silk protein was released respectively. However, during the second week, a burst protein release of glycerol mixed e-gel happened at day 9, when 47.8% (3:1), 82.7% (2:1), 74.0%（1:1）the silk protein was released respectively. On the contrary, a slow release curve of pure silk e-gel was observed. Only 25% silk protein is released at the end of 2 weeks.

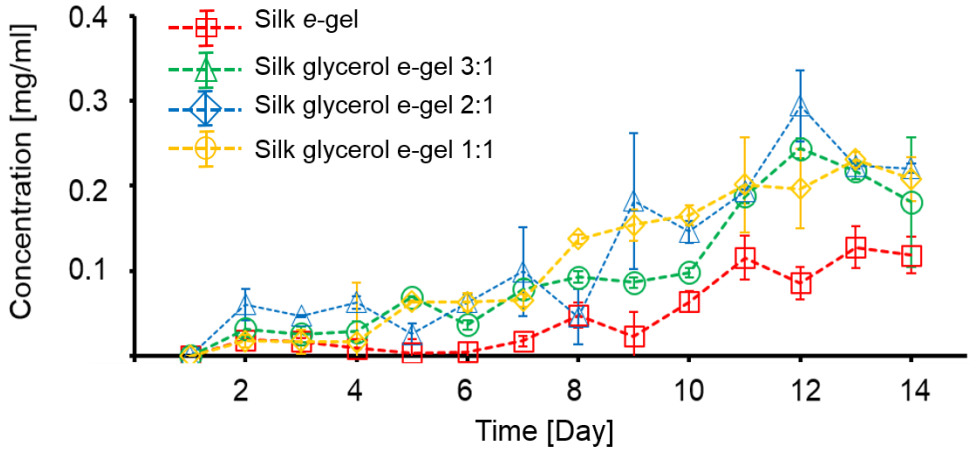

Fig 11. Long time storage assay. Silk *e*-gels were prepared with 3% silk solution. Silk egel (yellow curve), silk glycerol mixed *e*-gel at ratio 3:1 (red curve), silk glycerol mixed *e*-gel at ratio 2:1 (green curve) and silk glycerol mixed *e*-gel at ratio 1:1 (blue curve) were immersed in pH 2, 1M acetate acid buffer and at the temperature of 4 °C. Data is expressed as concentration of proteins via BCA assay (n = 3, error bar = standard deviation).

3.4. Silk *e*-gel *in vitro* drug loading

In order to investigate the applicability of silk *e*-gel as a drug delivery system, the positively charged, low molecular weight drug (doxorubicin) was loaded in silk *e*-gels via electrogelation. The volume of silk (200 μL), gelation time (30S), surface area of positive electrodes (113.04 mm^2), voltage (15V) and doxorubicin concentration (0.1mg/ml) were fixed. After gelation, Silk *e*-gels were dissolved in LiBr to release the doxorubicin. The loading behavior was studied with respect to the amount of the drug loaded to the total amount of drug added to silk solution before gelation. (Figure 12)

As Figure 12 indicates, loading efficiencies up to 25% were achieved at 15 V after pure silk gelation. The glycerol mixed silk e-gels had lower loading efficiencies (3:1, 23%; 2:1, 21%; 1:1, 15%) The loading efficiency of glycerol mixed silk *e*-gel decreased as the ratio of glycerol arose. One thing deserves notice is that during the electrogelation process, the ratio of silk did not influence loading ability much before the ratio 66%. However, 50% ratio of silk showed a substantial drop in loading efficiency (from 22% to less than 15%).

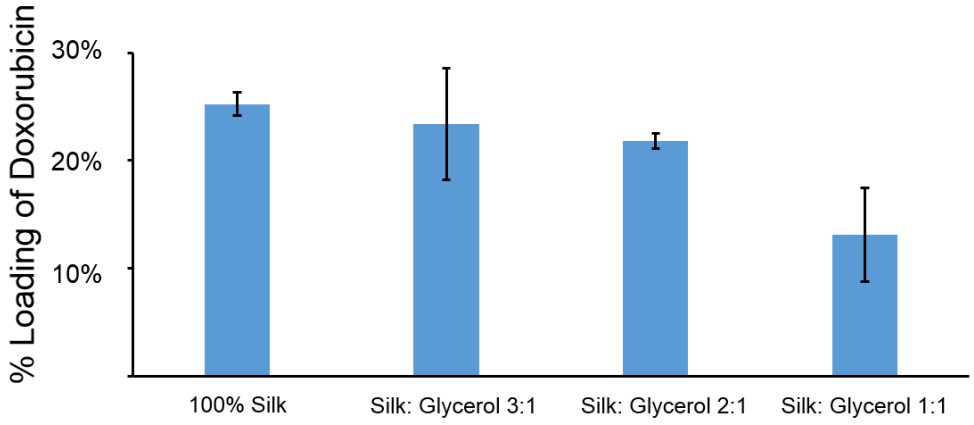

Fig. 12. Drug loading ability of silk *e*-gel. Silk egels were formed under determined conditions (15V, 30s gelation time, 0.1mg/ml doxorubicin, 113.04 mm^2 surface area of positive electrode and 200µL solution volume). Loading efficiencies of silk fibroin *e*-gels were calculated as released doxorubicin in LiBr solution with comparison to total doxorubicin added. Loading efficiencies of 25% (silk *e*-gel), 22%, (glycerol mixed *e*-gel at ratio 3:1), 20% (glycerol mixed *e*-gel at ratio 2:1), 15% (glycerol mixed *e*-gel at ratio 1:1) were achieved after electro gelation (n = 3, error bar = standard deviation).

3.5. Silk *e*-gel *in vitro* drug release

The in vitro release behavior of the drug from the silk e-gel in gastric juice (pH=2) was show in Figure 13. Doxorubicin, a drug frequently used in cancer chemotherapy and derived by chemical semi synthesis from a bacterial species, was selected as a drug for loading. The doxorubicin concentration at different time points in artificial gastric juice was detected via fluorescence at 595nm. The initial burst (cumulative release within the 4 hours) of all samples was 80%. Silk e-gel prepared from a 3% silk fibroin solution and loaded with doxorubicin showed a burst release of 72% within 75 minutes. On the other hand, although the different ratios of glycerol added to the silk did not influence doxorubicin release profile significantly, the silk e-gels mixed with glycerol which with higher silk II structure extended the release duration up to 4 hours compared to pure silk gel.

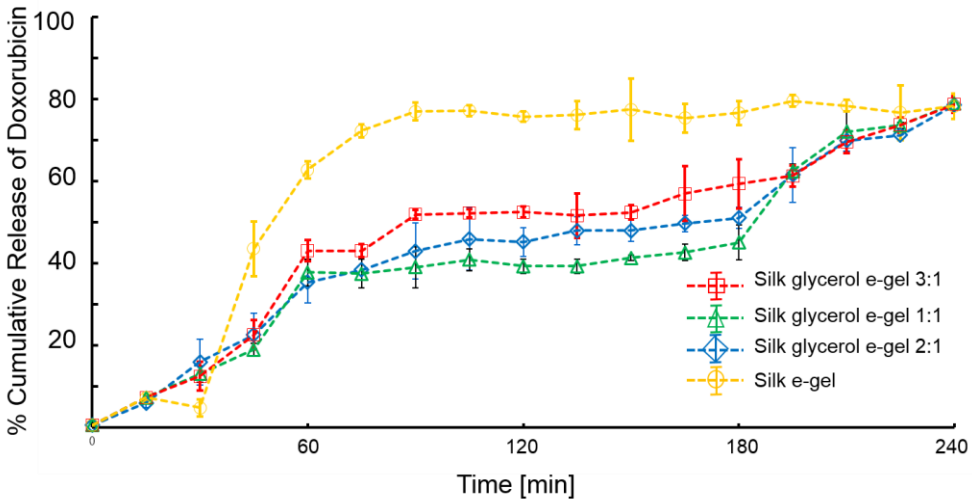

Fig 13. *In vitro* drug release behavior. Cumulative release of doxorubicin in 4 hours from silk egel, silk glycerol mixed *e*-gel at ratio 3:1, silk glycerol mixed *e*-gel at ratio 2:1 and silk glycerol mixed *e*-gel at ratio 1:1. Silk *e*-gels were prepared with 3% silk solution. Data is expressed as release ratio of doxorubicin relative to the negative controls which were totally dissolved in LiBr solution to calculate total amount of doxorubicin loaded in egels (n = 3, error bar = standard deviation).

3.6. Biocompatible and cytotoxicity assay.

A Good biocompatibly of a drug delivery vehicle is important for biomedical applications. The biocompatibly of silk e-gels was determined against N87 cells via AlamarBlue Assay. Similarly, in this experiment, electrogelation factors are fixed to ensure consistency. The cell viability of control groups of N87 cells which treated with PBS was regarded as 100% viability at each time point. As showed in Figure 14, all of the samples' cell viability was above 90% after 12 h incubation then dropped to below 80% in 48 h.

When cells were treated by doxorubicin encapsulated silk e-gels, cell viability was significantly decreased in comparison with e-gel controls without doxorubicin. 79%, 78%, 79% and 82% cell viability of N87 cells were achieved after 12h. A continuous and more evident decrease in cell viability was occurred by 48h with 39%, 42%, 43% and 41% respectively. Interestingly, glycerol mixed silk e-gels had similar cytotoxicity. Even at the ratio 1:1 (d), cell viability decreased to 41% at 48h.

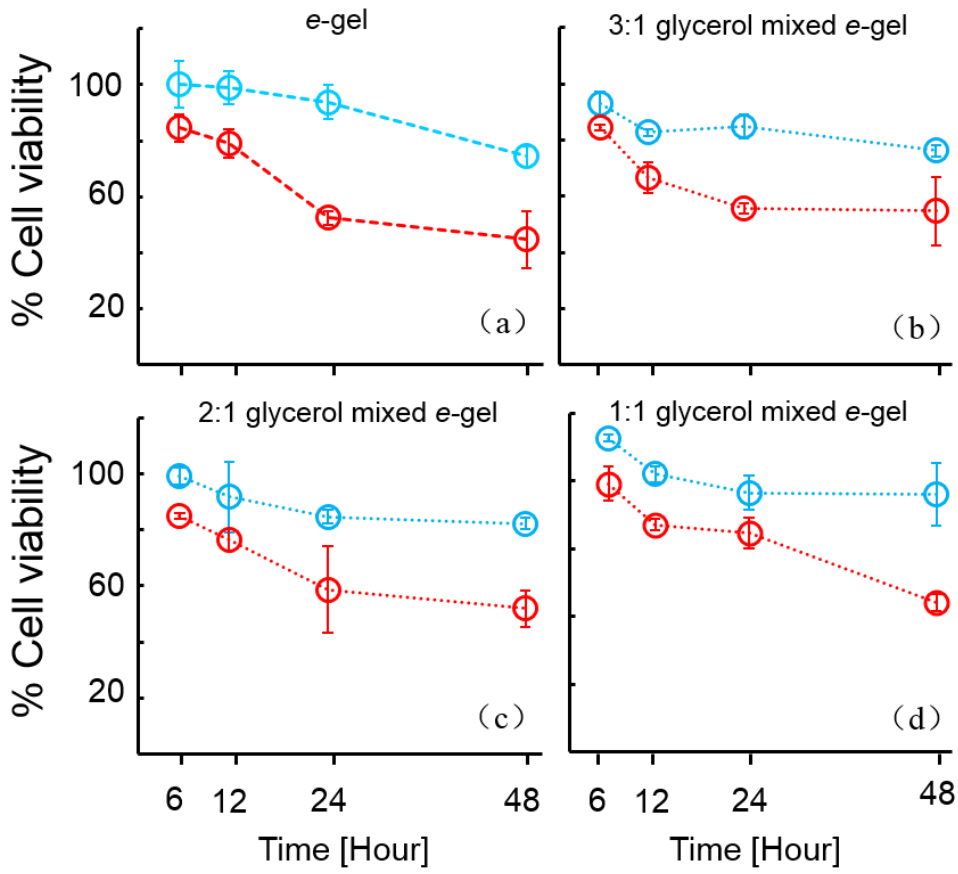

Fig. 14. Biocompatibly and cytotoxicity assay. Silk egels (blue curve) positive control and doxorubicin loaded silk *e*-gels (red curve) were incubated with NCI-N87 cells for up to 48 hours. The cell viability of control groups of N87 cells treated with PBS was considered as 100% viability at each time point. Cell proliferation was expressed as the percentage absorbance of samples relative to the negative control incubated with additional 200 µL PBS. Cell viability variation was obtained via co-culture with pure silk *e*-gel/doxorubicin loaded pure *e*-gel (a), silk glycerol mixed *e*-gel at ratio 3:1/ doxorubicin loaded silk glycerol mixed *e*-gel at ratio 3:1 (b), silk glycerol mixed *e*-gel at ratio 2:1/ doxorubicin loaded silk glycerol mixed *e*-gel at ratio 2:1 (c), silk glycerol mixed *e*-gel at ratio 1:1/ doxorubicin loaded silk glycerol mixed *e*-gel at ratio 1:1 (d) (n = 3, error bar = standard deviation).

3.7. Effect of doxorubicin on N87 cells

To further detect the morphological changes *e*-gel delivery system brought to N87 cells, doxorubicin at 0.1 mg/ml was encapsulated in silk *e*-gel/silk glycerol mixed *e*-gel and further applied to N87 cells. N87 cells treated with pure silk *e*-gel/silk glycerol mixed *e*-gels were placed as controls. The morphological of a large number of rhombic cells with the decrease of microvilli were observed (as showed in Figure 15) while the normal monolayer of dense epithelial colonies was recorded in control groups.

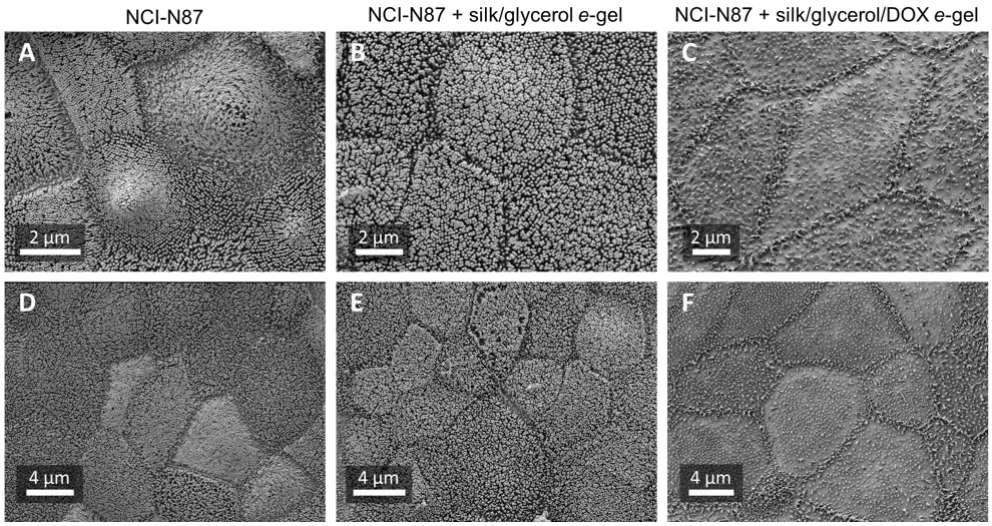

Fig 15. Morphology of N87 cells under treatment with doxorubicin loaded silk *e*-gels. The electron microscopic morphology was observed after 24 hours treatment. The morphology of the cells did not change from PBS treated control groups (A, D) to silk *e*-gel treated experimental groups with complete microvilli founding of N87 cells remained (B, E). The combination of doxorubicin with *e*-gel induced the decrease of cell microvilli in many cells, presented as cell transition from spherical cells to rhombic cells (C),and the disappearance of N87 microvilli (n=2).

3.8. Cellular uptake of doxorubicin

Due to the high drug loading capacity of silk *e*-gel and its doxorubicin-loaded cytotoxicity, the intracellular fate of doxorubicin loaded *e*-gels were monitored by fluoresce microscopy (Figure 16). The nucleus was stained with 4',6-diamidino-2-phenylindole (DAPI) in blue, doxorubicin was in red. At 2h of incubation, free doxorubicin accumulated was observed in cell nuclei. Doxorubicin loaded silk *e*-gel, however, partly accumulated the fluoresce signal of doxorubicin in the cytoplasm other than nuclei.

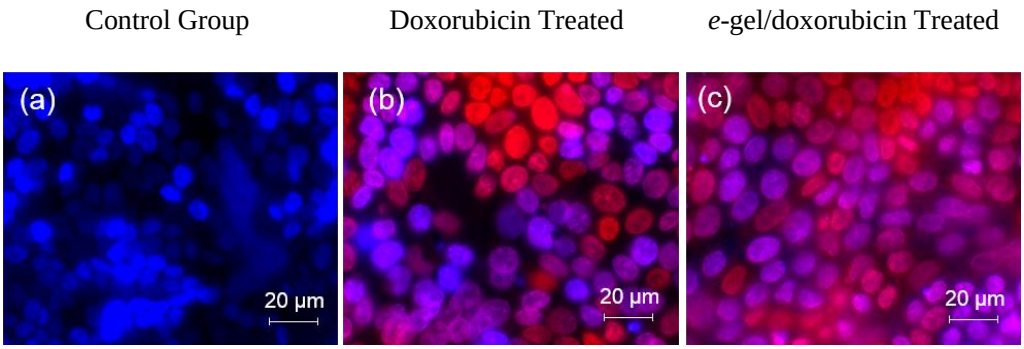

Fig 16. **Cellular uptake of doxorubicin/ doxorubicin loaded silk *e*-gels.** (a) 100% silk gel control 2h incubation. (b) 0.25 mg/ml free doxorubicin 2h incubation. (c) 100% silk *e*-gel loaded DOX 2h incubation. Nucleus was stained with DAPI (blue signal), doxorubicin was excited in red. The scale bar is 20µm. A clear view of nucleus was shown in Fig 14 (a) without doxorubicin signal. Free doxorubicin accumulated in cell nuclei at 2 hours in Figure 13 (b). Accumulated red doxorubicin loaded silk nanoparticles both in cytoplasm and in cell nuclei in figure 12 (c) after 2 hours incubation (n=6).

CHAPTER 4

DISCUSSIONS

Drug delivery in the stomach and controlled release can help in the treatment of stomach cancer and other related GI tract disease. For this approach, silk protein was a potential candidate due to its biocompatibility, biodegradability, and processing ability. In the present study, pH sensitive, short term silk drug release electro gels were prepared without any additional excipient, using an aqueous encapsulation process based on a low voltage gelation method at a controlled frequency and amplitude. Glycerol at different ratios were mixed with the silk solution to induce beta-sheet and enhance duration in gastric juice. This process had the advantages of being simple and scalable. In addition, this process could be carried out under very mild conditions, utilize only aqueous silk film solutions and work at room temperature, which is an appealing feature for the encapsulation of sensitive biologicals.

Earlier studies used silk films or other crystalized silk materials for drug delivery applications.[48] However, often months or years are needed to fully degrade the silk which limited its potential as short term drug release vehicles in the present study to gastric release.

Silk electro gel was a silk derived hydrogel that could reverse to solution in a short time period (<30 minutes in pH 7.0) .[8] Theoretically, a beta-sheet enhanced silk *e*-gel could elongate its release time in aqueous solution. Treatment with glycerol was selected as a beta-sheet induction method since it had been used to induce stabilized silk film, and accelerate silk gelation in our previous studies.[69] These earlier studies suggested that

glycerol was compatible with silk and offered an option for further study with respect to silk properties.

FTIR measurements confirmed that glycerol treated silk *e*-gels had an increase in beta-sheet content as indicated by a typical conformational shift in the amide I and amide II band regions when compared to untreated *e*-gels (Fig. 6, 7). This could be due to the fact that silk fibroin became densely packed and transferred to the crystal structure. Unlike former study [70], the beta-sheet structure dominated the glycerol mixed silk *e*-gels instead of alpha-helix. In particular, the lower ratio of glycerol (2:1) and (1:1) resulted in high ratio of beta-sheet (Figure 7). The higher ratio of glycerol on the other hand, had a significant peak of alpha-helix and random coil. These findings indicated the glycerol content in silk *e*-gels was important for the control of silk secondary structure transitions. During the silk e-gel electro gelation process, the glycerol molecule might interacts with silk fibroin chains via intermolecular forces, most likely hydrogen bonds between hydroxyl groups of glycerol and amide groups of silk.[69] This interaction alters the hydrophobic hydration state of silk protein chains and results in silk secondary structural change to from alpha-helix and random rich structure. According to a previous study, glycerol stabilized the helical stage of silk unless the film was treated by solvents. Given an aqueous environment, glycerol molecules bound to the silk fibroin chains would easily release.[70] The loss of glycerol would make the silk fibroin chains a more thermodynamically stable.[69] Similar mechanisms of silk structural transitions based on the change in hydrophobic hydration state of the protein chains were previously reported despite the fact that water molecule was replaced by glycerol.[71]

The DSC data, combined with TG data, gave a further insight of secondary structure transition in the manner of thermodynamic characteristics. The DSC curve of silk *e*-gel showed a crystallization peak between 200 and 215 ^{o}C, indicating that the structure was mainly amorphous. The amorphous silk transformed to beta-sheets above the glass transition temperature, Tg. On the other hand, the glycerol mixed silk *e*-gel did not show any crystallization peaks, indicating that the amorphous structures of silk in the fresh solution did not rearrange to form crystal structures, or the silk e-gel was fully crystallized. Interestingly, the decomposition temperature of silk *e*-gel decreased from 250 ^{o}C to less than 200 ^{o}C with glycerol mixtures. Similar trends also were noticed in TGA data. The glycerol mixed silk *e*-gels had lower thermo stability than the silk *e*-gel. The glycerol mixed silk e-gel with a high ratio of glycerol ratio had a higher decomposition temperature than those with lower glycerol ratio. This is understandable since FTIR data showed that high ratio glycerol silk *e*-gel was mostly similar to pure silk *e*-gel. The results also suggest the importance of the formation of intermediate structures for electrogelation, in good agreement with the FTIR data.

As expected, by adding glycerol to e-gel, the continuous process of silk e-gel gastric dissolvtion was extended from 90 minutes to four hours (Figure. 10). As a result, the release profile of doxorubicin was prolonged. (Figure. 13) This can result from the fact that an increase content of beta sheet happened in glycerol mixed silk e-gels, which enhanced the crosslink between silk fibroins. Although beta sheet changed the drug release profile of silk e-gel. The release was not governed by the ratio of glycerol added to silk solution, which indicated diffusion was the main release mechanism of doxorubicin.

High encapsulation efficiency was a desired feature of encapsulation technologies for controlled release. Higher encapsulation efficiency could minimize the loss of therapeutics, and help to extend the release rate. Our encapsulation process resulted in high encapsulation efficiencies in pure silk *e*-gel (25% of total amount of drug loaded in pure *e*-gel samples) in doxorubicin. However, the introduction of glycerol caused a major loss of drug loading capacity. The glycerol mixed *e*-gel dropped 22%, 20%, and 15% loading ability compared to pure silk *e*-gel (Fig 12). It is noteworthy that the loading ability showed nonlinear property to silk concentration. One reason that could explain this affinity is the different hydrophobicities of silk and doxorubicin. Silk had a pI of 4.2, due to the mainly negatively charged side chains of the hydrophilic spacers of the heavy chain.[42] Silk fibroin was likely to interact with the protonated amine group of doxorubicin (pKa= 8.2). Consequently, this affinity increased loading efficiency. The tightly packed silk network induced via glycerol might also contribute to the loading affinity. On the other hand, drug loading and release within the silk-based hydrogels could be altered by varying the degree of silk crystallinity as well.

Doxorubicin was used as a drug to investigate the release behavior of drug molecules from silk electro hydrogels in artificial gastric juice. The effects of hydrogel composition, mainly secondary changes, on in vitro drug release behavior of the composite hydrogels were investigated up to four hours. Hydrogels were mainly made up of water and thus generally have a large mesh size, which meant the most common mechanism of drug release from hydrogels is passive diffusion. Small molecules which had a molecular size less than the mesh size of the hydrogels could freely diffuse into/out of the hydrogel

matrix.[72] The size and characteristics of the solute, as well as the degree of crosslinking and the composition of the copolymers, influenced the release ability of the hydrogel matrix. Generally, either increasing the molecular weight of the solute or increasing the crosslinking density of the network would retard the release rate of the solute. The primary mechanism of drug release in silk hydrogel is generally considered diffusion since silk has no significant molecular level interactions with drug molecules. Moreover, weaker binding of doxorubicin molecules to the silk material also contributes to the significant initial quick release from the hydrogel matrix. As expected, a more tightly packed and beta-sheet rich structure resulted in a slower release rate of doxorubicin. Although the different ratio of glycerol seems to not significantly influence the release profile of doxorubicin *in vitro*.

Cell toxicity could be a matter of concern for a desired drug loading system. NCI-N87 cell line is an adequate cellular model exhibit epithelial morphology and are very useful in stomach cancer research. Cytotoxicity of e-gels in vitro was determined against NCL-N87 cells via AlamarBlue assay. Silk was normally considered as a biocompatible material, however, silk e-gels have little cytotoxicity in a 48h. The cytotoxicity happened may caused by the acid silk e-gel structure which lowered the cell medium's pH to the point below the optimal pH point for N87 cells. This cytotoxicity could be acceptable in a short term drug delivery system like a gastroretentive drug delivery system since most gastroretentive drug delivery systems would not exist in the stomach for more than 8 hours.[73] But the cytotoxicity might cause problems in longer term silk e-gel based drug delivery applications. Interestingly, glycerol induced silk e-gel resulted in a similar cytotoxicity curve during 48h assay. The uniform property of silk e-gel cytotoxicity hinted that the

difference of beta sheet did not affect the cytotoxicity of silk e-gel (Fig. 14). Future studies were needed to detail the mechanistic principles of e-gel cell toxicity mechanisms.

Delivery of doxorubicin via silk e-gel and silk glycerol mixed e-gel was confirmed effective in inhibiting the growth of N87 cancer cells via SEM and cell viability assays. The microvilli of doxorubicin treated N87 cells decreased significantly compared with control groups (Fig. 15). And 39%, 42%, 43% and 41% cell viability were reached after 48h incubation compared with untreated groups via AlamaBlue assay. Interestingly, both doxorubicin loaded silk *e*-gels and glycerol mixed silk *e*-gels at different ratios shared similar cytotoxicity curve during the 48h incubation (Fig. 14). These results indicated that beta sheet induction or the process of electrogelation affected the targeting ability or the activity of doxorubicin since the different loading efficacy influenced the doxorubicin loaded in e-gels.

A number of studies had shown that doxorubicin intercalates into DNA molecules.[74] The binding of doxorubicin to DNA inhibits DNA polymerase and nucleic acid synthesis. In addition, doxorubicin stabilizes the cleavable complex between DNA and topoisomerase II enzyme subunits, resulting in the formation of protein-linked DNA double-strand breaks.[74] Cellular uptake directly visualized the process of doxorubicin nuclei entrance. Doxorubicin loaded via *e*-gel was more likely in the cytoplasm than free doxorubicin which was accumulated in nuclei (Fig. 16). The nano-structure (microsphere) of silk e-gel was detected through SEM in further studies.[68] Endocytosis was considered as the mechanism for the absorbance of silk *e*-gel microspheres. The spherical aggregation small molecules absorbed by cell resulted in continuous drug release in the cell which may explain, at least

in part, why the doxorubicin loaded glycerol mixed silk had similar cytotoxicity compared to pure silk *e*-gel despite the difference of the amount of doxorubicin loaded.

CHAPTER 4

CONCLUSIONS

Silk electro hydrogel was selected as research candidate since it had several advantages like mild drug loading environment, pH sensitive dissolve profile, adhesive character, easily shaping by controlling the size of the positive electrodes as well as potential for further physical or genetical engineering improvements.

The overall goal of this study was to first determine whether silk electro hydrogel was suitable for a development of gsatrorentive drug delivery. The ability of pepsin to break down silk hydrogels is limited since silk hydrogel have a beta-sheet rich. In some biomedical applications, for example gastric drug delivery systems, short term and pH sensitive bio degradation/dissolvation character is desired. In the present study, an electrogelation method was used to form a novel silk electro gel system. The silk electro hydrogel was more susceptible to degradation in gastric juice than other forms of silk hydrogels in gastric juice since hydrogels had a lower beta-sheet (crystalline content).

The study was carried out with the silk electro hydrogels which can dissolve in artificial gastric juice in a short time. Glycerol was chosen as the beta-sheet inducer following previous studies.[70] It was found that silk e-gels have a pH sensitive dissolvtion rate in 1M acetate buffer, in the order of pH 8 > pH6 >pH2 (figure not included in this thesis). This corresponds to former papers which found that acidic environments stabilized silk e-gels.[75] Following long time storage study had shown silk *e*-gel remained stable after two week storage in pH 2 buffer, 4 ^{0}C. However, the existence of pepsin and other proteins

in gastric juice was shown significantly lowered the existence time of pure silk e-gel. The addition of glycerol was proved to stabilize silk e-gel in gastric juice further to 4 hours compared to pure silk e-gel, which could only exist for 90 minutes (Figure. 10).

The secondary structural changes in silk fibroin were considered as the main factor that influenced silk bio degradation profile.[29] The secondary structure transition during silk electrogelation and glycerol mixed silk electrogelation is summarized in Figures 7 and 8. These results indicated that the glycerol induced beta-sheet in all three experimental samples. In addition, the use of FSD allowed a clearer identification of some of these differences. In particular, the higher ratio of glycerol resulted in a lower ratio of beta-sheet (Figure. 7). Further DSC and TGA assay found glycerol impaired e-gels' thermostability and generated a more amorphous structure. These results fit our previous study that glycerol molecules interacted with silk fibroin chains via intermolecular forces, and might act as a plasticizer in the forming of silk e-gel (Figure. 7, 9). These findings provide the opportunity to explore how the secondary structure influences the profile of silk gastric degradation.

Doxorubicin, a drug used in cancer treatment, was loaded into silk e-gels. Silk e-gels performed well at encapsulating agents. The high ratio of drug loading capacity may be caused by the interaction between negatively charged silk fibroin and positively charged doxorubicin (Figure. 12). In the drug release experiment, silk/glycerol mixed silk *e*-gels released 80% of the drug before the end of four hours, which was three times slower than pure silk *e*-gel. These results are not unexpected since the beta sheet content to stabilized silk material in many situations including enzymatic digestion (Figure. 13).

In the following study, by adding doxorubicin loaded silk e-gels to human gastric cancer cells (N87 cells), significant weakened cell viability via AlamaBlue assay at time points 6h, 12h, 24h and 48h (Figure. 14) compared to the pure e-gel control groups as well as PBS treated control groups. To gain further insight into the overall cytotoxicity process, SEM and fluoresce microscope imaging were used. Doxorubicin loaded silk e-gel nanoparticles accumulated in the cell cytoplasm more than in the nuclei, which indicated that nanoparticles might enter cells via an endocytosis pathway, and hinted to a novel pathway to improve drug efficiency (Figure 16). In contrast, a significant decrease of cell microvilli was detected in doxorubicin treated groups in SEM imagining (Figure. 15), which showed that doxorubicin changed the cell phenotype after a 24 hour treatment.

We envisaged a silk *e*-gel based short term release system for delivering bioactive molecules in a pH sensitive manner. Silk *e*-gel showed potential for high drug loading capability and short term release profile in an acidic environment. The major advantages of the silk *e*-gel based drug delivery system we found it could be fabricated and loaded with an all aqueous process under mild conditions, and its degradation rate in the acid gastric environment could be adjusted via the variations of beta sheet content. Further, the intracellular drug release mechanism could help to improve efficiency.

CHAPTER 5

FUTURE WORK

A number of open questions must be solved to for a gastrorentive drug delivery system. These problems suggest a variety of experiment directions that need to be pursued.

5.1. Comparison study of different induction methods

The present study provided evidence that glycerol can extend the silk electro-gels gastric retention period. Structural analysis indicated the beta-sheet content may play the major role in the slow distribution rate of glycerol mixed silk *e*-gels. However, further characterization still needs to be performed on the study of silk e-gel gastric distribution. The glycerol ratio used in this study was 12.5%, 16.5% and 25%. It would be helpful if other ratios of glycerol (5%, 10%, 15%, 20%, 25%, 30%, 35%, 40%, 45%, 50%, 55%, 60%, 65%, 70%, 75%, 80%, 85%, 90%, 95%) are induced into the study. For example, up to 80% ratio of glycerol was used to induce alpha-helix in previous study.[70] A comparison study would help us better understanding the mechanism of silk electro gelation. Also, several of methods including methanol treatment,[35] high temperatures,[36] pH close to the isoelectric point of silk fibroin, the use of salts[37] and shear-force[38] were known to effectively induce the beta-sheet content in silk fibroin. The next investigation should be a complete comparison between those beta-sheet induction methods with the same electro gelation methods, and the same gastric dissolution methods described in this work. This comparison study should include a control group with pure silk *e*-gel control. All experimental groups should use the same one week aged 3 w/w% 10 minute boiled silk solution. The aim of this

comparison study is to investigate the influence of beta-sheet content on the silk e-gel's gastric distribution process.

DSC, TG and FTIR assays for the lyophilized silk *e*-gel samples should be performed to give a deep understanding of silk e-gels' secondary structure. The evaluation methods may include approaches like Fourier self-deconvolution and glass transition temperature analysis used in this work.

Expected results should be as following: Pure silk *e*-gel samples should rapidly dissolve in gastric juice, alpha-helix should dominate, and a decomposition temperature around 200 ^{0}C. The glycerol treated silk *e*-gels should have an extended gastric dissolve time, a higher ratio of beta-sheet content, and lower decomposition temperature. Other experimental groups should also have extended gastric dissolve time, a higher ratio of beta-sheet content but higher decomposition temperature.

5.2. Comparison study of different drugs' loading and release processes

Drug characteristics like molecular weight, molecular size, charge, hydrophilic or hydrophobic properties strongly influence the loading and release capacity in silk drug delivery studies [7]. Thus a study not only considers doxorubicin but also other frequently used ulcer and gastric cancer treating drugs like 5-fluorouracil,[76] ranitidine and amoxicillin[77] is desired to evaluate the silk e-gel as a drug delivery system. These experiments should include all four different drugs (including doxorubicin), and should follow the procedures mentioned in previous paragraphs in this study. Doxorubicin, due to its positively charged molecule, should attach to negatively charged silk fibroin and remain

high encapsulate capability, as well as slow release profile. However, those negatively charged or fewer positively charged drugs are expected to behave very differently compared with doxorubicin. For example, amoxicillin, which has a pI point of 5.4[78], has fewer positive electron compared to doxorubicin. This should result in less encapsulate capability and quick release profile. On the other hand, amoxicillin has a higher molecular weight compared to doxorubicin which should slow its release rate from silk hydrogel.

5.3. Additional cellular approaches to evaluate the effectiveness of silk *e*-gel drug release

The study has shown primary data of SEM and AlamarBlue assay which both indicated the cell viability of N87 cells were impaired during doxorubicin treatment *in vitro*. It would be preferable if a further study includes molecular-level experiment, which should show the metabolism transition of N87 cells during the drug treatment. For example, it is questionable if N87 cell apoptosis happened during doxorubicin treatment. Thus a tunnel assay is required.

Another molecular-level experiment should be HER2 expression detection. HER2 overexpression is increasingly recognized as a frequent molecular abnormality in gastric cancer study.[79] Trastuzumab (Herceptin) is a monoclonal antibody which specifically targets HER2 protein by directly binding the extracellular domain of the receptor.[79] Those Herceptin based ELISA, real-time PCR and immuno–staining should be applied to monitor the expression transition of HER2. Meanwhile, other gastric cancer specific gene markers like CA19-9[80] and HER2/neu[81] should also be studied in checked at protein level with

Western Blot assay.

5.4. *In vivo* test as a study for drug delivery approaches

The final goal is to develop an effective drug delivery approach based on the novel silk *e*-gel system. If the analysis mentioned above proved that the e-gel can deliver drug in gastric environment in a sustained way, we can then conduct some *in vivo* studies by applying drug loaded silk *e*-gel into animals. Different from *in vitro* applications, issues (gender, age, nation and numerous other issues) need to be considered for in vivo work.[82] The first concern of *in vivo* drug delivery systems always should be biocompatibility, Silk is a biocompatible material and it recently been approved by FDA for the application as a surgical mesh. Moreover, lately a 18 month *in vivo* adipose tissue regeneration experiment had shown long time scale stability and biocompatibility of silk materials.[83]

My particular interest would be the *in vivo* delivery method of silk *e*-gels. The silk electro gel system, like other hydrogel, is amorphous and lack of hardness. Under this condition, it is challenge to delivery silk *e*-gel itself to the stomach. pH sensitive material like chitosan which can capsulate silk *e*-gels and release them in the stomach could be one of the approaches that delivery our gastroretentive e-gel system.[84] However, this design is complex and hard to control. Based on the electrogelation property of silk solution, another more appropriate design should a specialized gastro scope system which equipped with containers of silk solution and drug, also with positive/negative electrodes. The gastro scope should find ulcer on the surface of the stomach in an intuitive way, and should deliver our silk *e*-gels as soon as it finds ulcer.

Other silk e-gel delivery approaches include a design called magnetic e-gel. In this design, magnetic metal atoms could loaded into silk fibroins via electro gelation process. The e-gel's motivation should be controlled by magnetic fields. This design could give a novel approach to control the e-gel system by applying magnetic fields outside the organ.

BIBLIOGRAPHY

1. Zuo, B.; Dai, L.; Wu, Z., Analysis of structure and properties of biodegradable regenerated silk fibroin fibers. *Journal of materials science* **2006,** *41* (11), 3357-3361.

2. Watanabe, T.; Tada, M.; Nagai, H.; Sasaki, S.; Nakao, M., Helicobacter pylori infection induces gastric cancer in mongolian gerbils. *Gastroenterology* **1998,** *115* (3), 642-8.

3. Jemal, A.; Bray, F.; Center, M. M.; Ferlay, J.; Ward, E.; Forman, D., Global cancer statistics. *CA: a cancer journal for clinicians* **2011,** *61* (2), 69-90.

4. Cid, T. P.; Fernandez, M. C.; Benito Martinez, S.; Jones, N. L., Pathogenesis of Helicobacter pylori infection. *Helicobacter* **2013,** *18 Suppl 1*, 12-7.

5. Lin, Y. S.; Chen, M. J.; Shih, S. C.; Bair, M. J.; Fang, C. J.; Wang, H. Y., Management of Helicobacter pylori infection after gastric surgery. *World journal of gastroenterology : WJG* **2014,** *20* (18), 5274-82.

6. Lovenish Bhardwaj, P. K. S., Rishabha Malviya, A Short Review on Gastro Retentive Formulations *African Journal of Basic & Applied Sciences* **2011**.

7. Wenk, E.; Merkle, H. P.; Meinel, L., Silk fibroin as a vehicle for drug delivery applications. *Journal of controlled release : official journal of the Controlled Release Society* **2011,** *150* (2), 128-41.

8. Leisk, G. G.; Lo, T. J.; Yucel, T.; Lu, Q.; Kaplan, D. L., Electrogelation for protein adhesives. *Advanced materials* **2010,** *22* (6), 711-5.

9. Ping Zhou, G. L., Zhengzhong Shao, Xiaoyun Pan, and Tongyin Yu, Structure of Bombyx mori Silk Fibroin Based on the DFT Chemical Shift Calculation
J. Phys. Chem. B **2001,** (105
), 12469-12476.

10. Mirvish, S. S., The etiology of gastric cancer. Intragastric nitrosamide formation and other theories. *Journal of the National Cancer Institute* **1983,** *71* (3), 629-47.

11. Siegel, R.; Naishadham, D.; Jemal, A., Cancer statistics, 2013. *CA: a cancer journal for clinicians* **2013,** *63* (1), 11-30.

12. Kantarjian, H.; Koller, C. A.; Wolff, R. A., *The MD Anderson manual of medical oncology*. McGraw-Hill, Medical Pub.: 2006.

13. Zabaleta, J., Multifactorial etiology of gastric cancer. In *Cancer Epigenetics*, Springer: 2012; pp 411-435.

14. Jemal, A.; Center, M. M.; DeSantis, C.; Ward, E. M., Global patterns of cancer incidence and mortality rates and trends. *Cancer Epidemiology Biomarkers & Prevention* **2010,** *19* (8), 1893-1907.

15. Schistosomes, liver flukes and Helicobacter pylori. IARC Working Group on the Evaluation of Carcinogenic Risks to Humans. Lyon, 7-14 June 1994. *IARC Monogr Eval Carcinog Risks Hum* **1994,** *61*, 1-241.

16. Parsonnet, J.; Friedman, G. D.; Vandersteen, D. P.; Chang, Y.; Vogelman, J. H.; Orentreich, N.; Sibley, R. K., Helicobacter pylori infection and the risk of gastric carcinoma. *New England Journal of Medicine* **1991,** *325* (16), 1127-1131.

17. Lin, J. T.; Wang, L. Y.; Wang, J. T.; Wang, T. H.; Yang, C. S.; Chen, C. J., A nested case-control study on the association between Helicobacter pylori infection and gastric cancer risk in a cohort of 9775 men in Taiwan. *Anticancer Res* **1995,** *15* (2), 603-6.

18. Correa, P.; Piazuelo, M. B., The gastric precancerous cascade. *J Dig Dis* **2012,** *13* (1), 2-9.
19. Alwan, A., *Global status report on noncommunicable diseases 2010*. World Health Organization: 2011.
20. Moore, R. J.; Spiegel, D., *Cancer, culture, and communication*. Springer: 2004.
21. Fried, T. R.; Bradley, E. H.; Towle, V. R.; Allore, H., Understanding the treatment preferences of seriously ill patients. *New England Journal of Medicine* **2002,** *346* (14), 1061-1066.
22. Eldridge, B., Chemotherapy and nutrition implications. *The Clinical Guide to Oncology Nutrition. Chicago, Ill: The American Dietetic Association* **2000**, 61-9.
23. Lim, L.; Michael, M.; Mann, G. B.; Leong, T., Adjuvant therapy in gastric cancer. *Journal of clinical oncology* **2005,** *23* (25), 6220-6232.
24. Wagner, A. D.; Grothe, W.; Haerting, J.; Kleber, G.; Grothey, A.; Fleig, W. E., Chemotherapy in advanced gastric cancer: a systematic review and meta-analysis based on aggregate data. *Journal of Clinical Oncology* **2006,** *24* (18), 2903-2909.
25. Talukder, R.; Fassihi, R., Gastroretentive delivery systems: a mini review. *Drug development and industrial pharmacy* **2004,** *30* (10), 1019-1028.
26. Moes, A., Gastroretentive dosage forms. *Critical reviews in therapeutic drug carrier systems* **1992,** *10* (2), 143-195.
27. Malafaya, P. B.; Silva, G. A.; Reis, R. L., Natural–origin polymers as carriers and scaffolds for biomolecules and cell delivery in tissue engineering applications. *Advanced drug delivery reviews* **2007,** *59* (4), 207-233.
28. Mano, J.; Silva, G.; Azevedo, H. S.; Malafaya, P.; Sousa, R.; Silva, S.; Boesel, L.; Oliveira, J. M.; Santos, T.; Marques, A., Natural origin biodegradable systems in tissue engineering and regenerative medicine: present status and some moving trends. *Journal of the Royal Society Interface* **2007,** *4* (17), 999-1030.
29. Vepari, C.; Kaplan, D. L., Silk as a biomaterial. *Progress in polymer science* **2007,** *32* (8), 991-1007.
30. McGrath, K.; Kaplan, D., *Protein-based materials*. Springer: 1997.
31. (a) Ha, S.-W.; Gracz, H. S.; Tonelli, A. E.; Hudson, S. M., Structural study of irregular amino acid sequences in the heavy chain of Bombyx mori silk fibroin. *Biomacromolecules* **2005,** *6* (5), 2563-9; (b) Lu, Q.; Zhu, H.; Zhang, C.; Zhang, F.; Zhang, B.; Kaplan, D. L., Silk self-assembly mechanisms and control from thermodynamics to kinetics. *Biomacromolecules* **2012,** *13* (3), 826-832.
32. Bini, E.; Knight, D. P.; Kaplan, D. L., Mapping domain structures in silks from insects and spiders related to protein assembly. *Journal of molecular biology* **2004,** *335* (1), 27-40.
33. Trefiletti, V.; Conio, G.; Pioli, F.; Cavazza, B.; Perico, A.; Patrone, E., The spinning of silk, 1. Molecular weight, subunit structure, and molecular shape of bombyx mori fibroin. *Die Makromolekulare Chemie* **1980,** *181* (6), 1159-1179.
34. Valluzzi, R.; Jin, H.-J., X-ray evidence for a "super"-secondary structure in silk fibers. *Biomacromolecules* **2004,** *5* (3), 696-703.
35. (a) Freiberg, S.; Zhu, X., Polymer microspheres for controlled drug release. *International journal of pharmaceutics* **2004,** *282* (1), 1-18; (b) Monti, P.; Freddi, G.; Bertoluzza, A.; Kasai, N.; Tsukada, M., Raman spectroscopic studies of silk fibroin from Bombyx mori. *Journal of Raman spectroscopy* **1998,** *29* (4), 297-304; (c) Marsh, R. E.; Corey, R. B.; Pauling, L., An

investigation of the structure of silk fibroin. *Biochimica et Biophysica Acta* **1955,** *16*, 1-34.
36. Ishida, M.; Asakura, T.; Yokoi, M.; Saito, H., Solvent-and mechanical-treatment-induced conformational transition of silk fibroins studies by high-resolution solid-state carbon-13 NMR spectroscopy. *Macromolecules* **1990,** *23* (1), 88-94.
37. Zong, X.-H.; Zhou, P.; Shao, Z.-Z.; Chen, S.-M.; Chen, X.; Hu, B.-W.; Deng, F.; Yao, W.-H., Effect of pH and copper (II) on the conformation transitions of silk fibroin based on EPR, NMR, and Raman spectroscopy. *Biochemistry* **2004,** *43* (38), 11932-11941.
38. Jin, H.-J.; Kaplan, D. L., Mechanism of silk processing in insects and spiders. *Nature* **2003,** *424* (6952), 1057-1061.
39. Jin, H. J.; Park, J.; Karageorgiou, V.; Kim, U. J.; Valluzzi, R.; Cebe, P.; Kaplan, D. L., Water‐Stable Silk Films with Reduced β‐Sheet Content. *Advanced Functional Materials* **2005,** *15* (8), 1241-1247.
40. Wenk, E.; Wandrey, A. J.; Merkle, H. P.; Meinel, L., Silk fibroin spheres as a platform for controlled drug delivery. *Journal of Controlled Release* **2008,** *132* (1), 26-34.
41. Tanaka, T.; Magoshi, J.; Magoshi, Y.; ichi Inoue, S.; Kobayashi, M.; Tsuda, H.; Becker, M.; Nakamura, S., Thermal properties of bombyx mori and several wild silkworm silks Phase transition of liquid silk. *Journal of thermal analysis and calorimetry* **2002,** *70* (3), 825-832.
42. Li, M.; Lu, S.; Wu, Z.; Yan, H.; Mo, J.; Wang, L., Study on porous silk fibroin materials. I. Fine structure of freeze dried silk fibroin. *Journal of applied polymer science* **2001,** *79* (12), 2185-2191.
43. Lanza, R.; Langer, R.; Vacanti, J. P., *Principles of tissue engineering*. Academic press: 2011.
44. Numata, K.; Cebe, P.; Kaplan, D. L., Mechanism of enzymatic degradation of beta-sheet crystals. *Biomaterials* **2010,** *31* (10), 2926-2933.
45. Altman, G. H.; Diaz, F.; Jakuba, C.; Calabro, T.; Horan, R. L.; Chen, J.; Lu, H.; Richmond, J.; Kaplan, D. L., Silk-based biomaterials. *Biomaterials* **2003,** *24* (3), 401-416.
46. Wang, Y.; Rudym, D. D.; Walsh, A.; Abrahamsen, L.; Kim, H.-J.; Kim, H. S.; Kirker-Head, C.; Kaplan, D. L., < i> In vivo</i> degradation of three-dimensional silk fibroin scaffolds. *Biomaterials* **2008,** *29* (24), 3415-3428.
47. Tang, X.; Ding, F.; Yang, Y.; Hu, N.; Wu, H.; Gu, X., Evaluation on in vitro biocompatibility of silk fibroin‐based biomaterials with primarily cultured hippocampal neurons. *Journal of Biomedical Materials Research Part A* **2009,** *91* (1), 166-174.
48. Pritchard, E. M.; Kaplan, D. L., Silk fibroin biomaterials for controlled release drug delivery. *Expert opinion on drug delivery* **2011,** *8* (6), 797-811.
49. Matsumoto, A.; Chen, J.; Collette, A. L.; Kim, U.-J.; Altman, G. H.; Cebe, P.; Kaplan, D. L., Mechanisms of silk fibroin sol-gel transitions. *The Journal of Physical Chemistry B* **2006,** *110* (43), 21630-21638.
50. Cao, Y.; Wang, B., Biodegradation of silk biomaterials. *International journal of molecular sciences* **2009,** *10* (4), 1514-1524.
51. Kim, U.-J.; Park, J.; Li, C.; Jin, H.-J.; Valluzzi, R.; Kaplan, D. L., Structure and properties of silk hydrogels. *Biomacromolecules* **2004,** *5* (3), 786-792.
52. Pritchard, E. M.; Szybala, C.; Boison, D.; Kaplan, D. L., Silk fibroin encapsulated powder reservoirs for sustained release of adenosine. *Journal of Controlled Release* **2010,** *144* (2), 159-167.

53. Wang, X.; Wenk, E.; Hu, X.; Castro, G. R.; Meinel, L.; Wang, X.; Li, C.; Merkle, H.; Kaplan, D. L., Silk coatings on PLGA and alginate microspheres for protein delivery. *Biomaterials* **2007,** *28* (28), 4161-4169.

54. Wang, X.; Hu, X.; Daley, A.; Rabotyagova, O.; Cebe, P.; Kaplan, D. L., Nanolayer biomaterial coatings of silk fibroin for controlled release. *Journal of Controlled release* **2007,** *121* (3), 190-199.

55. Ambrose, E.; Elliott, A., Infra-red spectra and structure of fibrous proteins. *Proceedings of the Royal Society of London. Series A. Mathematical and Physical Sciences* **1951,** *206* (1085), 206-219.

56. Kim, U.-J.; Park, J.; Joo Kim, H.; Wada, M.; Kaplan, D. L., Three-dimensional aqueous-derived biomaterial scaffolds from silk fibroin. *Biomaterials* **2005,** *26* (15), 2775-2785.

57. Hu, X.; Kaplan, D.; Cebe, P., Determining beta-sheet crystallinity in fibrous proteins by thermal analysis and infrared spectroscopy. *Macromolecules* **2006,** *39* (18), 6161-6170.

58. Hu, X.; Kaplan, D.; Cebe, P., Effect of water on the thermal properties of silk fibroin. *Thermochimica Acta* **2007,** *461* (1), 137-144.

59. Seib, F. P.; Pritchard, E. M.; Kaplan, D. L., Self‐Assembling Doxorubicin Silk Hydrogels for the Focal Treatment of Primary Breast Cancer. *Advanced functional materials* **2013,** *23* (1), 58-65.

60. Du, Y.; Xu, Y.; Ding, L.; Yao, H.; Yu, H.; Zhou, T.; Si, J., Down-regulation of miR-141 in gastric cancer and its involvement in cell growth. *Journal of gastroenterology* **2009,** *44* (6), 556-561.

61. Chang, K.-J.; Chen, C.-N.; Juan, H.-F.; Tseng, C.-W., Method for determining the prognosis of gastric cancer. Google Patents: 2009.

62. Xia, X.-X.; Wang, M.; Lin, Y.; Xu, Q.; Kaplan, D. L., Hydrophobic Drug-Triggered Self-Assembly of Nanoparticles from Silk-Elastin-Like Protein Polymers for Drug Delivery. *Biomacromolecules* **2014,** *15* (3), 908-914.

63. Lin, Y.; Xia, X.; Shang, K.; Elia, R.; Huang, W.; Cebe, P.; Leisk, G.; Omenetto, F.; Kaplan, D. L., Tuning Chemical and Physical Cross-Links in Silk Electrogels for Morphological Analysis and Mechanical Reinforcement. *Biomacromolecules* **2013,** *14* (8), 2629-2635.

64. (a) Byler, D. M.; Susi, H., Examination of the secondary structure of proteins by deconvolved FTIR spectra. *Biopolymers* **1986,** *25* (3), 469-487; (b) Jung, C., Insight into protein structure and protein-ligand recognition by Fourier transform infrared spectroscopy. *J Mol Recognit* **2000,** *13* (6), 325-51.

65. Griffiths, P. R.; De Haseth, J. A., *Fourier transform infrared spectrometry*. John Wiley & Sons: 2007; Vol. 171.

66. (a) Mouro, C.; Jung, C.; Bondon, A.; Simonneaux, G., Comparative Fourier transform infrared studies of the secondary structure and the CO heme ligand environment in cytochrome P-450cam and cytochrome P-420cam. *Biochemistry* **1997,** *36* (26), 8125-34; (b) Goormaghtigh, E.; Cabiaux, V.; Ruysschaert, J. M., Secondary structure and dosage of soluble and membrane proteins by attenuated total reflection Fourier-transform infrared spectroscopy on hydrated films. *Eur J Biochem* **1990,** *193* (2), 409-20; (c) Jackson, M.; Mantsch, H. H., The use and misuse of FTIR spectroscopy in the determination of protein structure. *Critical reviews in biochemistry and molecular biology* **1995,** *30* (2), 95-120.

67. Tretinnikov, O. N.; Ohta, K., Conformation-sensitive infrared bands and conformational

characteristics of stereoregular poly (methyl methacrylate) s by variable-temperature FTIR spectroscopy. *Macromolecules* **2002,** *35* (19), 7343-7353.

68. Lu, Q.; Huang, Y.; Li, M.; Zuo, B.; Lu, S.; Wang, J.; Zhu, H.; Kaplan, D. L., Silk fibroin electrogelation mechanisms. *Acta biomaterialia* **2011,** *7* (6), 2394-400.

69. Hanawa, T.; Watanabe, A.; Tsuchiya, T.; Ikoma, R.; Hidaka, M.; Sugihara, M., New oral dosage form for elderly patients: preparation and characterization of silk fibroin gel. *Chem Pharm Bull (Tokyo)* **1995,** *43* (2), 284-8.

70. Lu, S.; Wang, X.; Lu, Q.; Zhang, X.; Kluge, J. A.; Uppal, N.; Omenetto, F.; Kaplan, D. L., Insoluble and flexible silk films containing glycerol. *Biomacromolecules* **2009,** *11* (1), 143-150.

71. Banga, A. K.; Chien, Y. W., Hydrogel-based lontotherapeutic delivery devices for transdermal delivery of peptide/protein drugs. *Pharmaceutical research* **1993,** *10* (5), 697-702.

72. Ta, H. T.; Dass, C. R.; Dunstan, D. E., Injectable chitosan hydrogels for localised cancer therapy. *Journal of Controlled Release* **2008,** *126* (3), 205-216.

73. Garg, S.; Sharma, S., Gastroretentive drug delivery systems. **2003**.

74. Tacar, O.; Sriamornsak, P.; Dass, C. R., Doxorubicin: an update on anticancer molecular action, toxicity and novel drug delivery systems. *J Pharm Pharmacol* **2013,** *65* (2), 157-70.

75. Kojic, N.; Panzer, M. J.; Leisk, G. G.; Raja, W. K.; Kojic, M.; Kaplan, D. L., Ion Electrodiffusion Governs Silk Electrogelation. *Soft matter* **2012,** *8* (26), 2897-2905.

76. Maehara, Y., S-1 in gastric cancer: a comprehensive review. *Gastric Cancer* **2003,** *6 Suppl 1*, 2-8.

77. Hentschel, E.; Brandstatter, G.; Dragosics, B.; Hirschl, A. M.; Nemec, H.; Schutze, K.; Taufer, M.; Wurzer, H., Effect of ranitidine and amoxicillin plus metronidazole on the eradication of Helicobacter pylori and the recurrence of duodenal ulcer. *New England Journal of Medicine* **1993,** *328* (5), 308-312.

78. Féria, C.; Ferreira, E.; Correia, J. D.; Gonçalves, J.; Caniça, M., Patterns and mechanisms of resistance to β-lactams and β-lactamase inhibitors in uropathogenic Escherichia coli isolated from dogs in Portugal. *Journal of Antimicrobial Chemotherapy* **2002,** *49* (1), 77-85.

79. Gravalos, C.; Jimeno, A., HER2 in gastric cancer: a new prognostic factor and a novel therapeutic target. *Annals of Oncology* **2008,** *19* (9), 1523-1529.

80. Wobbes, T.; Thomas, C.; Segers, M.; Nagengast, F., Evaluation of seven tumor markers (CA 50, CA 19‐9, CA 19‐9 TruQuant, CA 72‐4, CA 195, carcinoembryonic antigen, and tissue polypeptide antigen) in the pretreatment sera of patients with gastric carcinoma. *Cancer* **1992,** *69* (8), 2036-2041.

81. Cortés-Funes, H.; Rivera, F.; Alés, I.; Márquez, A.; Velasco, A.; Colomer, R.; Garcia-Carbonero, R.; Sastre, J.; Guerra, J.; Gravalos, C., Phase II of trastuzumab and cisplatin in patients (pts) with advanced gastric cancer (AGC) with HER2/neu overexpression/amplification. *J Clin Oncol* **2007,** *25* (18S), 4613.

82. Lavan, D. A.; McGuire, T.; Langer, R., Small-scale systems for in vivo drug delivery. *Nature biotechnology* **2003,** *21* (10), 1184-1191.

83. Bellas, E.; Panilaitis, B. J.; Glettig, D. L.; Kirker-Head, C. A.; Yoo, J. J.; Marra, K. G.; Rubin, J. P.; Kaplan, D. L., Sustained volume retention< i> in vivo</i> with adipocyte and lipoaspirate seeded silk scaffolds. *Biomaterials* **2013,** *34* (12), 2960-2968.

84. Risbud, M. V.; Hardikar, A. A.; Bhat, S. V.; Bhonde, R. R., pH-sensitive freeze-dried chitosan–polyvinyl pyrrolidone hydrogels as controlled release system for antibiotic delivery.

Journal of controlled release **2000,** *68* (1), 23-30.